

AD-A054 145

NAVAL ACADEMY ANNAPOLIS MD DEPT OF MECHANICAL ENGINEERING F/G 13/10
ANALOG SIMULATION OF A WAVE ACTIVATED TURBINE GENERATOR BUOY. (U)

JAN 76 R A HIRSCH

MIPR-Z70099-5-54326-A

UNCLASSIFIED

EW-9-75

USCG-D-57-76

NL

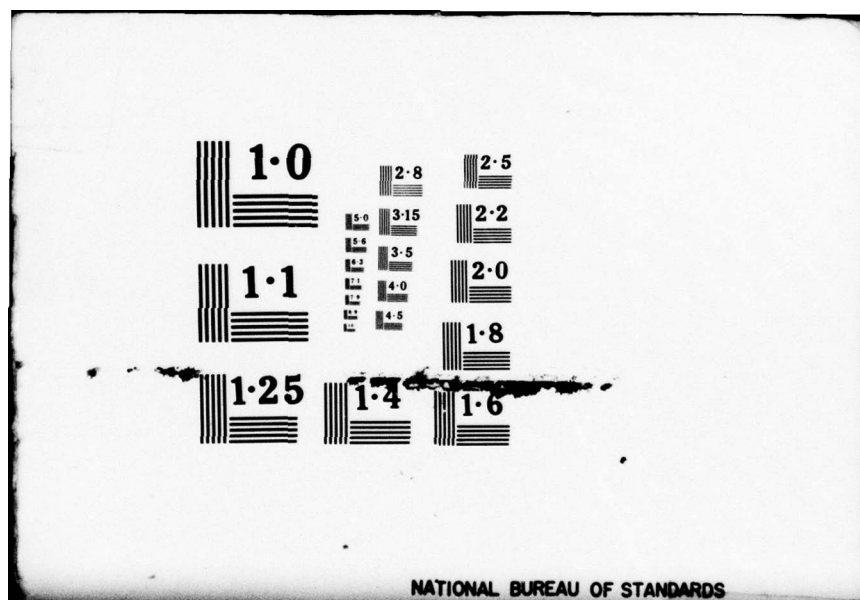
1 OF 1
ADA
054145



The microfiche contains 60 frames of technical information, organized into a grid of 5 rows and 12 columns. The frames contain various types of content, including:

- Textual descriptions and specifications.
- Block diagrams and circuit schematics.
- Graphs and plots, including a prominent one in the third row, third column.
- Tables of data.
- Photographs of physical components.
- Flowcharts and process diagrams.

END
DATE
FILMED
6-78
DDC



NATIONAL BUREAU OF STANDARDS

FOR FURTHER TRAN



art
12

AD A 054145

Report No. CG-D-57-76

ANALOG SIMULATION OF A WAVE ACTIVATED
TURBINE GENERATOR BUOY

RICHARD A. HIRSCH, P.E.



JANUARY 1976

FINAL REPORT

DDC
RECEIVED
MAY 23 1978
B

AD No. []
DDC FILE COPY

Document is available to the U. S. public through the
National Technical Information Service,
Springfield, Virginia 22161

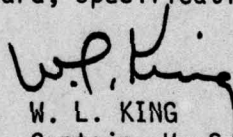
Prepared for
U. S. DEPARTMENT OF TRANSPORTATION
UNITED STATES COAST GUARD
Office of Research and Development
Washington, D.C. 20590

NOTICE

This document is disseminated under the sponsorship of the Department of Transportation in the interest of information exchange. The United States Government assumes no liability for its contents or use thereof.

The United States Government does not endorse products or manufacturers. Trade or manufacturers' names appear herein solely because they are considered essential to the object of this report.

The contents of this report do not necessarily reflect the official view or policy of the U. S. Coast Guard and do not constitute a standard, specification, or regulation.



W. L. KING
Captain, U. S. Coast Guard
Chief, Environmental and
Transportation Technology Division
Office of Research and Development
U. S. Coast Guard
Washington, D. C. 20590

Technical Report Documentation Page

<p>1. Report No. CG-D-57-76</p>	<p>2. Government Accession No.</p>	<p>3. Recipient's Catalog No.</p>	
<p>4. Title and Subtitle Analog Simulation of a Wave Activated Turbine Generator Buoy</p>		<p>5. Report Date January 1976</p>	<p>6. Performing Organization Code</p>
<p>7. Author(s) Richard A. Hirsch P.E.</p>	<p>12. 78p.</p>	<p>8. Performing Organization Report No. EW-9-75</p>	<p>10. Work Unit No. (TRAIS)</p>
<p>9. Performing Organization Name and Address U. S. Naval Academy Annapolis, Maryland <i>see next p.</i></p>		<p>11. Contract or Grant No. MIPR-770099-5-54326-A</p>	<p>13. Type of Report and Period Covered FINAL REPORT</p>
<p>12. Sponsoring Agency Name and Address Office of Research and Development U. S. Coast Guard Washington, D.C. 20590</p>		<p>14. Sponsoring Agency Code G-DET-2</p>	
<p>15. Supplementary Notes</p>			
<p>16. Abstract This report presents an analog simulation of a Wave Activated Turbine Generator Buoy which is currently under study and evaluation by the U. S. Coast Guard. Emphasis is placed upon the theoretical development since only limited full scale data is available. However, based upon the available data, the author does suggest some areas in which program modifications probably will be required.</p>			
<p>17. Key Words Energy, Natural Energy Sources, Wave Energy Conversion</p>		<p>18. Distribution Statement Document is Available to the Public through the National Technical Information Service, Springfield, Virginia, 22161</p>	
<p>19. Security Classif. (of this report) Unclassified</p>	<p>20. Security Classif. (of this page) Unclassified</p>	<p>21. No. of Pages 75</p>	<p>22. Price</p>

407 358

LB

Preface

NR This report is taken directly from U. S. Naval Academy Report EW-9-75 entitled "Analog Simulation of a Wave Activated Turbine Generator Buoy." It was authored by Prof. Richard A. Hirsch of the Mechanical Engineering Department under MIPR No. Z-70099-5-54326-A. It describes Prof. Hirsch's analytical development of the subject simulation.

ACCESSION for		
NTIS	White Section	<input checked="" type="checkbox"/>
DDC	Buff Section	<input type="checkbox"/>
UNANNOUNCED		<input type="checkbox"/>
JUSTIFICATION		
BY		
DISTRIBUTION/AVAILABILITY CODES		
Dist.	AVAIL and/or	SPECIAL
<i>A</i>		

SUMMARY

This report presents an analog simulation model of a Wave Activated Turbine Generator Buoy which is currently under study and evaluation by the United States Coast Guard. The equations describing the heaving dynamics are developed as well as the equations describing the output of the air operated turbine/generator subsystem. The equations are scaled for analog computation and the computer patching diagrams are presented.

Although only limited full scale data was available, an analysis of this data indicates that the model developed will probably require modification. Final conclusions as to the modifications required must await further full scale data. For this reason, analog computer results are not presented at this time.

TABLE OF CONTENTS

	<u>Page</u>
1. INTRODUCTION	1
2. WAVE EXCITATION	4
3. WATER COLUMN MOTION EQUATION	11
4. BUOY MOTION EQUATION	14
5. AIR COLUMN ANALYSIS	21
6. TURBINE TORQUE	30
7. TURBINE/GENERATOR EQUATIONS	36
8. ANALOG SIMULATION	39
9. VALIDATION OF THE SIMULATION MODEL	65
10. CONCLUSIONS AND RECOMMENDATIONS	71
REFERENCES	72

1. INTRODUCTION

The Wave Activated Turbine Generator (WATG) has been under study and evaluation by the U. S. Coast Guard for some time. The basic concept has been described and analyzed by McCormick in References 1, 2, and 3. A typical configuration is shown in Figure 1-1.

Wave action causes heaving motion of both the buoy and central water column. In general, these heaving motions are of different amplitudes and phase thus inducing relative motion of the air above the water column. The air is forced through nozzles in the turbine stator and causes the turbine rotor to rotate. The turbine rotor is directly coupled to the rotor of a generator producing an alternating current output. This output is converted to direct current which is used to charge the batteries which operate the various navigation aids.

The prior analyses have been concerned with the effect of various system parameters, associated with the buoy and water column, on the power available to the turbine as a result of given sinusoidal wave inputs of known frequency and amplitude. These analyses all have the following features:

- . The system output is determined as the power available to the turbine.
- . The power available is computed from the unsteady motion of incompressible air in a straight air passage with a single head loss.
- . The air motion is determined by the relative motion of the buoy and internal free surface and does not affect these motions.
- . The buoy and water column are each treated as uncoupled, viscously damped, linear oscillators forced by sinusoidal waves of different amplitudes but the same frequency and phase.
- . The input wave motion is unaffected by the motions of the buoy and water column.

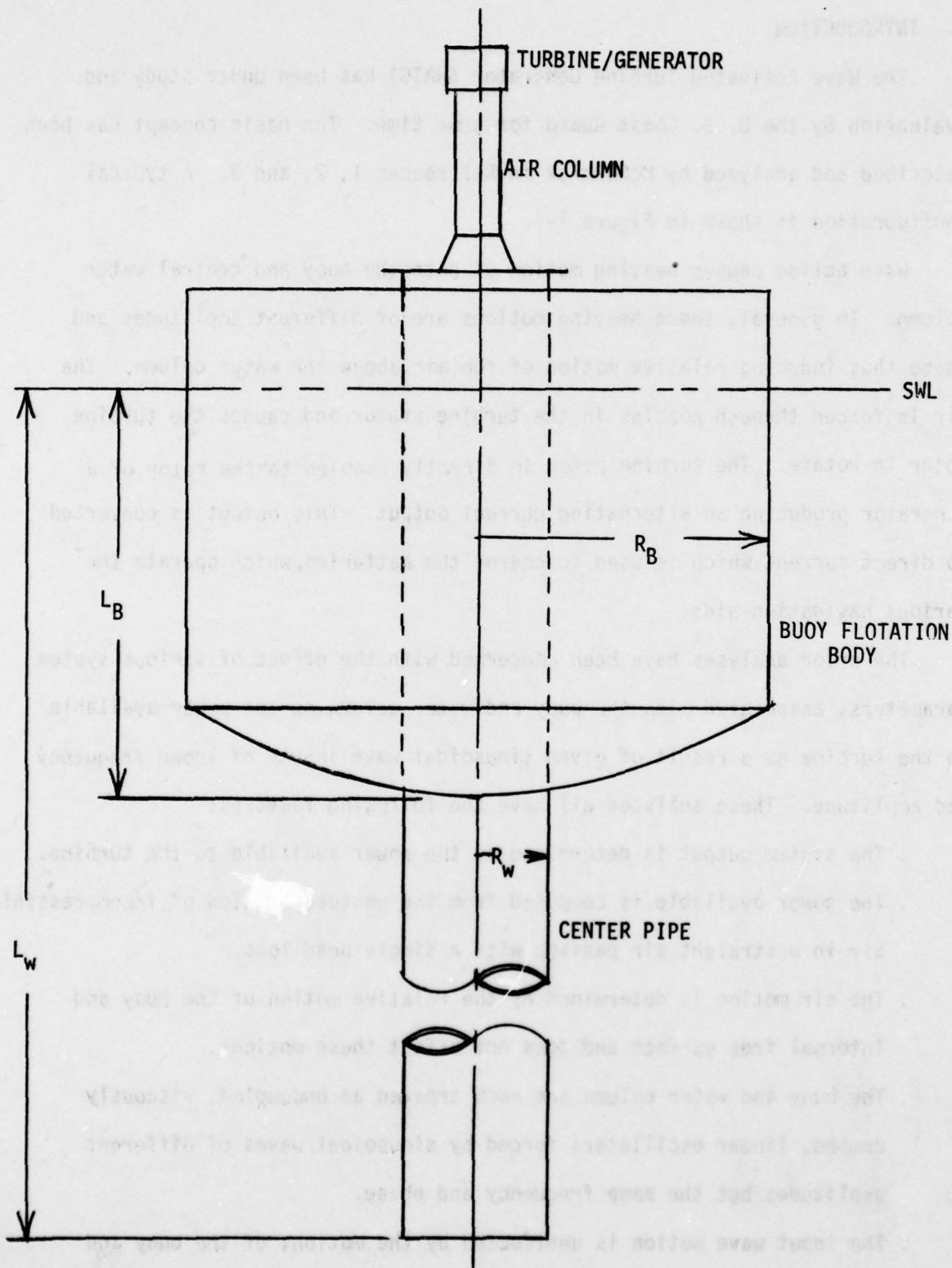


FIGURE 1-1. TYPICAL WATG CONFIGURATION

The results reported in References 1-3 are useful for identifying significant parameters and in predicting general trends. For example, Figure 5 of Reference 2 indicates that more energy is dissipated during the relative rising of the water column than during the relative falling. In addition, Reference 3 points out that the power available is strongly dependent upon the values of the damping coefficients estimated. Full scale test data is necessary in order to identify the actual energy dissipation mechanisms inherent in the system. Such tests have been initiated by the U. S. Coast Guard but data is not yet available.

The study reported herein was undertaken in anticipation of the fact that the prior linear analysis may prove to be inadequate and also to include the turbine, generator, and air passage in the simulation. Specifically, the objectives were:

- . To model the buoy and water column as a coupled system including all significant non-linear effects.
- . To model the actual air passage of the hardware under test.
- . To model the turbine and generator.
- . To present the model in a form suitable for solution on an analog computer.
- . To analyze any full scale data that becomes available and modify the model if necessary.

Chapters 2 - 8 present the detailed development of the simulation model. Chapter 9 presents the analysis of available full scale data and the conclusions and recommendations resulting from this study are presented in Chapter 10.

2. WAVE EXCITATION

2.1 Background

The excitation imposed by a seaway on a floating body is difficult to determine except in the case of simple bodies. The first simplifying assumption made is known as the Froude - Kryloff hypothesis which states that the presence of the body does not affect the pressure field of the surrounding wave system. This hypothesis has been found to give good results for floating bodies and, hence, should be applicable herein. The second simplifying assumption is known as the St. Dennis - Pierson hypothesis which states that the response of the body to a sum of wave components is the same as the sum of its responses to each wave component. This hypothesis has been found to give good results in relatively low sea states and, hence, should be applicable to the buoys under study which are generally located in semi-protected waters. Based upon these assumptions, the response of the buoy system to random waves of small amplitude can be found by the superposition in random phase of responses to steady state sinusoidal wave inputs. Therefore, the present study will concentrate on determining the system response to a single, sinusoidal wave pattern derived from classical, linearized wave theory. Such waves are known as Airy waves and are analyzed in Reference 4, and the results are summarized herein.

2.2 Airy Waves

The solution of the linearized wave equation, due to Airy, results in waves of sinusoidal profile and is applicable to waves of small amplitude occurring in deep water. The profile is given by

$$\eta(x,y,t) = \eta_M \cos \beta(x,y,t)$$

where

$$\eta_M = \text{wave amplitude at the surface} = H/2$$

$$H = \text{wave height}$$

$$\beta(x, y, t) = \text{phase angle} = k(x \cos\alpha) + k(y \sin\alpha) - \sigma t$$

$$k = \text{wave number} = \frac{2\pi}{\lambda} = \frac{\omega^2}{g}$$

$$\lambda = \text{wavelength} = \frac{gT^2}{2\pi} = \frac{2\pi g}{\omega^2}$$

ω = wave frequency

g = gravitational acceleration

α = wave heading

σ = frequency of encounter

t = time

T = wave period = $2\pi/\omega$

The coordinate system is defined in Figure 2-1.

In this study, the buoy has a vertical axis of symmetry and all incoming waves will be assumed to have the same heading and hence, $\alpha = 0$. Also, since the buoy is not underway, $\sigma = \omega$, so

$$\eta(x, y, t) = \eta_M \cos(kx - \omega t)$$

Furthermore, according to the Airy theory, the water particle orbital motion is attenuated at any depth z and this attenuation is given by

$$\eta_z = \eta_M \frac{\cosh k(z + d)}{\sinh kd}$$

where

$$d = \text{depth to the sea bottom}$$

For the Airy theory to apply, the depth, d , must be at least half the wavelength.

Now

$$\cosh k(z + d) = \cosh kz \cosh kd + \sinh kz \sinh kd$$

and

$$kd = 2\pi \frac{d}{\lambda}$$

and if

$$\frac{d}{\lambda} > \frac{1}{2}$$

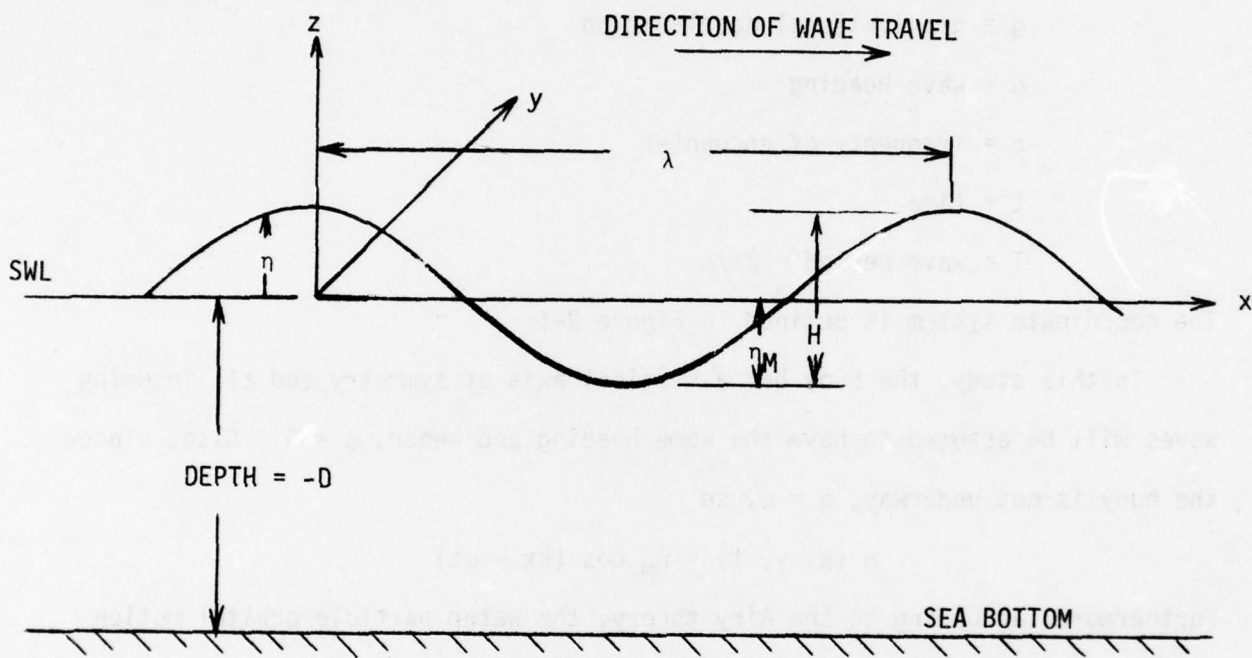


FIGURE 2-1. AIRY WAVE SYSTEM

then

$$kd > \pi$$

and

$$\sinh kd = \cosh kd$$

within 1/2 %, so

$$\eta_z = \eta_M (\cosh kz + \sinh kz)$$

But

$$\sinh kz = \frac{1}{2} (e^{kz} - e^{-kz})$$

and

$$\cosh kz = \frac{1}{2} (e^{kz} + e^{-kz})$$

so

$$\eta_z = \eta_M e^{kz}$$

and, finally

$$\eta = \frac{H}{2} e^{-kD} \cos (kx - \omega t) \quad (2-1)$$

where

D = distance below the still water line

Equation (2-1) is the final form of the wave profile used in this study and is used to determine the pressure field and thus the forces exerted by the wave on the floating body. Since the wave profile is a function of the coordinate x , the pressure on the body has to be integrated over the body in order to determine the total force. An example of this integration follows.

2.3 Integration Of The Wave Pressure

Employing the Froude - Kryloff hypothesis, the pressure on the floating body due to the wave is

$$p_n = \rho g \eta$$

where

ρ = fluid mass density

In the present study only vertical motion of the buoy - water column system is considered and if the submerged elements are assumed to have straight, vertical sides, the total upward force is found by integrating p_η over the appropriate area in the x-y plane at depth D. For example, for an annular body with inside radius r and outside radius R, with draft D, as shown in Figure 2-2, the total vertical force F_z is:

$$F_z = \int p_\eta dA = \rho g \frac{H}{2} e^{-kD} \int \cos(kx - \omega t) dA$$

Now

$$x = r \cos\theta$$

$$dA = r dr d\theta$$

so

$$F_z = \rho g \frac{H}{2} e^{-kD} \int_0^{2\pi} \int_r^R \cos(kr \cos\theta - \omega t) r dr d\theta$$

This integration has been demonstrated in Reference 1 and proceeds as follows:

$$\cos x = \frac{1}{2} (e^{ix} + e^{-ix})$$

so

$$\cos(kr \cos\theta - \omega t) = \frac{1}{2} (e^{-i\omega t} e^{ikr \cos\theta} + e^{i\omega t} e^{-ikr \cos\theta})$$

and from Reference 5, page 355

$$J_n(z) = \frac{i^{-n}}{\pi} \int_0^\pi e^{iz \cos\theta} d\theta$$

where

$$J_n(z) = \text{Bessel function of the first kind of order } n$$

so

$$\int_0^{2\pi} e^{ikr \cos\theta} d\theta = 2\pi J_0(kr)$$

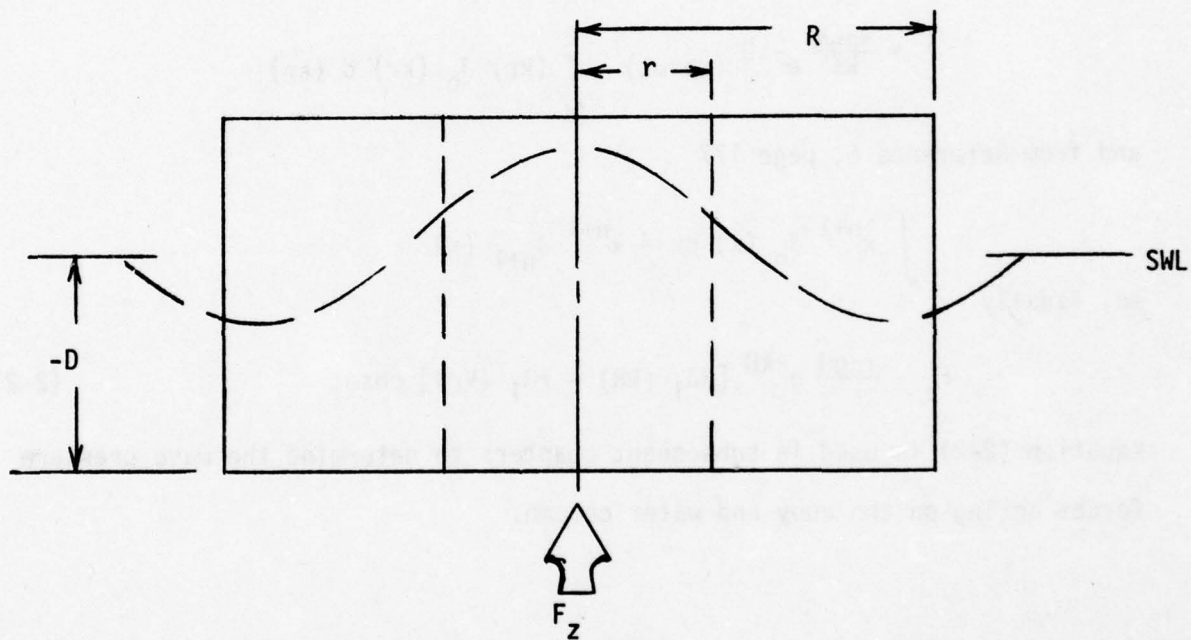


FIGURE 2-2. ANNULAR FLOTATION BODY

$$\int_0^{2\pi} e^{-ikr\cos\theta} d\theta = 2\pi J_0(-kr)$$

but, from Reference 5, page 353

$$J_0(-kr) = J_0(kr)$$

so

$$\begin{aligned} F_z &= \rho g \frac{H}{2} e^{-kD} \int_r^R \pi (e^{-i\omega t} + e^{i\omega t}) J_0(kr) dr \\ &= \frac{\pi \rho g H}{k^2} e^{-kD} (\cos \omega t) \int_r^R (kr) J_0(kr) d(kr) \end{aligned}$$

and from Reference 6, page 177

$$\int x^{n+1} J_n(x) dx = x^{n+1} J_{n+1}(x)$$

so, finally

$$F_z = \frac{\pi \rho g H}{k} e^{-kD} [R J_1(kR) - r J_1(kr)] \cos \omega t \quad (2-2)$$

Equation (2-2) is used in subsequent chapters to determine the wave pressure forces acting on the buoy and water column.

3. WATER COLUMN MOTION EQUATION

3.1 Introduction

At rest in still water, the length of the water column in the center pipe (Figure 1-1) is L_W and assuming that the pipe has a constant radius R_W , its cross sectional area is $A_W = \pi R_W^2$, then the initial mass of water is

$$m_W = \rho A_W L_W$$

If the vertical motion is referenced to the SWL (still water line) and is measured positive upward, let z_W be the absolute vertical displacement of the water column and z_B be the absolute vertical displacement of the buoy and pipe, then at any time, the mass of water in motion within the pipe is

$$m_W = \rho A_W (L_W + z_W - z_B)$$

and its absolute acceleration is \ddot{z}_W , so $\rho A_W (L_W + z_W - z_B) \ddot{z}_W = \text{SUM OF VERTICAL FORCES (POSITIVE UP)}$

The vertical forces acting are:

$p_{nw} A_W =$ wave pressure force at the bottom of the water column (acting up)

$-\rho g A_W z_W =$ weight of water displaced from static equilibrium (acting down)

$-p_{aw} A_W =$ air pressure force at the free surface of the water column (acting down)

$D_{WB} =$ friction force at the pipe/water internal interface (opposing the relative velocity)

Expressions for these forces are developed herein.

3.2 Wave Pressure Force

The wave pressure force acting at the bottom of the center pipe opening is directly derivable from Equation 2-2 with

$$r = 0$$

$$R = R_W$$

$$J_1(0) = 0$$

$$D = L_W - z_B$$

so

$$p_{\eta W} A_W = \frac{\pi \rho g H R_W J_1(k R_W)}{k} e^{-k(L_W - z_B)} \cos \omega t$$

3.3 Friction Force

The frictional force due to the relative motion of the water in the pipe is assumed to be derivable from the Darcy-Weissbach equation for pressure loss in a pipe due to fluid viscosity. From Reference 7, page 417, this pressure loss is

$$\Delta p = \frac{f \rho \bar{u}^2 L}{2D} = \frac{4L}{D} \tau_o$$

where

f = friction factor

ρ = fluid mass density

l = pipe length

D = pipe length

\bar{u} = average fluid velocity (over the cross section)
relative to the pipe

τ_o = shear stress on pipe wall (acting on the wetted area $2\pi RL$)

For the water column

$$R = R_W$$

$$L = L_W + z_W - z_B$$

$$\bar{u} = \dot{z}_B - \dot{z}_W$$

and

$$D_{WB} = 2\pi RL \tau_o = \pi R^2 \Delta p$$

so

$$D_{WB} = \frac{\pi \rho f}{4} R_W (L_W + z_W - z_B) (\dot{z}_B - \dot{z}_W) |(\dot{z}_B - \dot{z}_W)|$$

where the velocity-squared term is written as shown in order to give the force the proper sign opposing the relative velocity. For example, when $\dot{z}_W > \dot{z}_B$ the water is moving up relative to the pipe and the force on the

water is down or negative. For turbulent flow in a moderately rough pipe the value of f would be 0.020.

3.4 Equation of Motion

Combining the results of the previous sections the equation of motion for the water column is

$$\begin{aligned} \rho A_W (L_W + z_W - z_B) \ddot{z}_W = & -\rho g A_W z_W - p_{aw} A_W \\ & + \frac{\pi \rho f}{4} (L_W + z_W - z_B) R_W (\dot{z}_B - \dot{z}_W) |(\dot{z}_B - \dot{z}_W)| \\ & + \frac{\pi \rho g H R_W^2 J_1(k R_W)}{k} e^{-k(L_W - z_B)} \cos \omega t \end{aligned} \quad (3-1)$$

The air pressure force, $-p_{aw} A_W$, will be developed further in Chapter 5.

4. BUOY MOTION EQUATION

4.1 Introduction

The buoy is assumed to execute pure heaving motion and thus the equation of motion is

$$m_B \ddot{z}_B = \Sigma \text{ vertical hydrodynamic forces} - D_{wB} + p_{aB} A_B$$

where D_{wB} is the force due to friction in the center pipe (developed in Chapter 3) and $p_{aB} A_B$ is the air pressure force to be developed in Chapter 5. The hydrodynamic forces arise from pressures due to the displacement, velocity, and acceleration associated with both the buoy motion and the wave motion. Following the exposition of Reference 4, these forces can be identified as:

WDF = wave displacement force

BDF = buoy displacement force

WAF = wave acceleration force

BAF = buoy acceleration force

VF = velocity forces due to wave and buoy

Expressions for these forces are developed herein, based upon Reference 4.

4.2 Wave Displacement Force

The wave displacement force in the vertical (z) direction is found from

$$WDF = \iiint \frac{\partial p_n}{\partial z} d\tau$$

where $d\tau$ is a volume element and the integration is over the submerged volume. If it is assumed that the buoy flotation body is an annulus with straight sides and inside radius R_w and outside radius R_B , and that the pressure on the center pipe thickness can be neglected, the above integral reduces to that given previously in Chapter 2. The resulting force is

$$WDF = \frac{\pi \rho g H}{k} e^{-k(L_B - z_B)} \left[R_B J_1(kR_B) - R_w J_1(kR_w) \right] \cos \omega t$$

where L_B is the draft of the buoy's flotation collar.

4.3 Buoy Displacement Force

The buoy displacement force is that resulting from changes in displacement from the static equilibrium position.

$$BDF = -\rho g A_B z_B$$

4.4 Wave Acceleration Force

The wave acceleration force is derived from

$$WAF = \iiint \rho C_h \frac{\partial^2 \eta}{\partial t^2} dV$$

where C_h is the hydrodynamic inertia (added mass) coefficient in heave. If it is assumed that C_h is not a function of (x, y, z) or that some mean value is used, then

$$WAF = \rho C_h \frac{\partial^2}{\partial t^2} \iiint \eta dV = \rho C_h D \frac{d^2}{dt^2} \left(\frac{F_z}{\rho g} \right)$$

where F_z is given in Chapter 2, The final form is

$$WAF = -\frac{\pi \rho H C_h D \omega^2}{k} e^{-k(L_B - z_B)} \left[R_B J_1(kR_B) - R_W J_1(kR_W) \right] \cos \omega t$$

4.5 Buoy Acceleration Force

The force due to buoy acceleration is

$$BAF = -\rho \nabla C_h \ddot{z}_B$$

but since $\nabla = A_B (L_B - z_B)$

$$BAF = -\rho A_B C_h (L_B - z_B) \ddot{z}_B$$

4.6 Velocity Forces due to Wave and Buoy

All of the velocity forces are due to relative velocity between the buoy and the wave. There are three distinct types of velocity forces to consider; friction force, pressure force, and radial dissipation or wavemaking force.

4.6.1 Friction force, D_f

Fluid viscosity gives rise to a shear force on the external vertical surface of the buoy which is proportional to the wetted area and the square of the relative velocity. This force is generally much smaller than the other velocity forces and hence it will be neglected.

$$D_f = 0$$

4.6.2 Pressure force, D_p

This force is due to the dynamic pressure acting on the cross-sectional area normal to the flow. The general form is

$$D_p = \frac{1}{2} \rho C_D A v^2$$

The area normal to the vertical flow is A_B and the relative normal velocity at the location of this area is

$$v = \dot{\eta} - \dot{z}_B \quad \text{at depth} - L_B$$

From Chapter 2

$$\dot{\eta} = \frac{\omega H}{2} e^{-k(L_B - z_B)} \sin(kr \cos\theta - \omega t)$$

In order to preserve the proper sign for this force, it must change sign when the relative velocity changes sign. It is also to be noted that since the buoy is only partially submerged, the proper drag coefficient is the forebody drag coefficient when the relative velocity is positive and the base drag coefficient when the relative velocity is negative. In view of the foregoing

$$D_p = \frac{1}{2} \rho A_B v^2 C_D \operatorname{sgn} v$$

Now, since $\dot{\eta}$ varies over the area (it is a function of x, y) an integration over the area must be carried out, so that

$$\frac{D_p}{\frac{1}{2} \rho C_D (\operatorname{sgn} v)} = \int_{R_w}^{R_B} \int_0^{2\pi} (\dot{\eta} - \dot{z}_B)^2 r dr d\theta = I$$

or

$$I = \iint \dot{n}^2 r dr d\theta - 2\dot{z}_B \iint \dot{n} r dr d\theta + \dot{z}_B^2 \iint r dr d\theta$$

or

$$I = I_1 - 2\dot{z}_B I_2 + \dot{z}_B^2 I_3$$

These integrals are now evaluated.

4.6.2.1 evaluation of I_3

$$I_3 = \int_{R_W}^{R_B} \int_0^{2\pi} r dr d\theta = A_B = \pi (R_B^2 - R_W^2)$$

4.6.2.2 evaluation of I_2

$$I_2 = \frac{\omega H}{2} e^{-k(L_B - z_B)} \int_{R_W}^{R_B} \int_0^{2\pi} \sin(kr \cos\theta - \omega t) r dr d\theta$$

but

$$\begin{aligned} \sin(kr \cos\theta - \omega t) &= \frac{1}{2i} \left[e^{i(kr \cos\theta - \omega t)} - e^{-i(kr \cos\theta - \omega t)} \right] \\ &= \frac{e^{-i\omega t}}{2i} e^{ikr \cos\theta} - \frac{e^{i\omega t}}{2i} e^{-ikr \cos\theta} \end{aligned}$$

so

$$\begin{aligned} I_2 &= \frac{\omega H}{2} e^{-k(L_B - z_B)} \int_{R_W}^{R_B} r dr \int_0^{2\pi} \left[\frac{e^{-i\omega t}}{2i} e^{ikr \cos\theta} - \frac{e^{i\omega t}}{2i} e^{-ikr \cos\theta} \right] d\theta \\ &= \frac{\omega H}{2} e^{-k(L_B - z_B)} \int_{R_W}^{R_B} 2\pi \frac{e^{-i\omega t} - e^{i\omega t}}{2i} J_0(kr) r dr \\ &= -\frac{\pi \omega H}{k^2} e^{-k(L_B - z_B)} (\sin \omega t) \int_{R_W}^{R_S} kr J_0(kr) d(kr) \end{aligned}$$

and finally

$$I_2 = -\frac{\pi\omega H}{k} e^{-k(L_B - z_B)} [R_B J_1(kR_B) - R_W J_1(kR_W)] \sin\omega t$$

4.6.2.3 evaluation of I_1

$$I_1 = \left[\frac{\omega H}{2} e^{-k(L_B - z_B)} \right]^2 \int_{R_W}^{R_B} \int_0^{2\pi} \sin^2(kr\cos\theta - \omega t) r dr d\theta$$

but

$$\begin{aligned} \sin^2(kr\cos\theta - \omega t) &= -\frac{1}{4} \left[e^{2i(kr\cos\theta - \omega t)} + e^{-2i(kr\cos\theta - \omega t)} - 2 \right] \\ &= \frac{1}{2} - \frac{e^{-2i\omega t}}{4} e^{2ikr\cos\theta} - \frac{e^{2i\omega t}}{4} e^{-2ikr\cos\theta} \end{aligned}$$

so

$$\begin{aligned} \left[\frac{\omega H}{2} e^{-k(L_B - z_B)} \right]^2 &= \frac{1}{2} A_B - \frac{\pi \cos 2\omega t}{(2k)^2} \int_{R_W}^{R_B} (2kr) J_0(2kr) d(2kr) \\ &= \frac{1}{2} A_B - \frac{\pi}{2k} [R_B J_1(2kR_B) - R_W J_1(2kR_W)] \cos 2\omega t \end{aligned}$$

and finally

$$I_1 = \frac{1}{2} \left[\frac{\omega H}{2} e^{-k(L_B - z_B)} \right]^2 \left\{ A_B - \frac{\pi}{k} [R_B J_1(2kR_B) - R_W J_1(2kR_W)] \cos 2\omega t \right\}$$

The final form of the pressure force is

$$D_p = \frac{1}{2\rho} (I_1 - 2\dot{z}_B I_2 + \dot{z}_B^2 I_3) (C_D \operatorname{sgn} v)$$

where

$$\operatorname{sgn} v = \left| -\frac{\pi\omega H}{kA_B} e^{-k(L_B - z_B)} [R_B J_1(kR_B) - R_W J_1(kR_W)] \sin\omega t - \dot{z}_B \right|$$

and I_1, I_2, I_3 are as above.

4.6.3 Radial dissipation force, D_R

This force is generated by the energy carried away by the waves created by the oscillating buoy. For a hull with a vertical axis of symmetry and straight sides, the radial dissipation generated by a section of unit length is

$$\frac{4\rho\omega}{k^2} (\sin^2ky) e^{-2k(L_B - z_B)} (\dot{\eta} - \dot{z}_B)$$

where y is the half-width of the section and

$$\dot{\eta} = \frac{\omega H}{2} e^{-k(L_B - z_B)} \sin(kx - \omega t)$$

The total force is then

$$D_R = \frac{4\rho\omega}{k^2} e^{-2k(L_B - z_B)} \int (\sin^2ky) \left[\frac{\omega H}{2} e^{-k(L_B - z_B)} \sin(kx - \omega t) - \dot{z}_B \right] dx$$

where the integration is over the length in the x -direction and, in general, y is a function of x . This integration could not be carried out exactly for the case at hand where the water plane area is circular. The integral can be approximated by replacing the buoy waterplane with an equivalent area rectangle of width w and length L such that

$$y = \frac{w}{2} = R_B \quad \text{and} \quad L = \frac{A_B}{2R_B}$$

Proceeding with this approximation

$$\begin{aligned} D_R &= \frac{4\rho\omega}{k^2} e^{-2k(L_B - z_B)} \sin^2kR_B \int_{-L/2}^{L/2} \left[\frac{\omega H}{2} e^{-k(L_B - z_B)} \sin(kx - \omega t) - \dot{z}_B \right] dx \\ &= \frac{4\rho\omega}{k^2} e^{-2k(L_B - z_B)} \sin^2kR_B \left\{ -\frac{\omega H}{2k} e^{-k(L_B - z_B)} \left[\cos\left(\frac{kL}{2} - \omega t\right) - \cos\left(\frac{kL}{2} + \omega t\right) \right] - L\dot{z}_B \right\} \\ D_R &= -\frac{4\rho\omega}{k^2} e^{-2k(L_B - z_B)} (\sin^2kR_B) \left[\frac{\omega H}{k} e^{-k(L_B - z_B)} \sin\frac{kA_B}{4R_B} \sin\omega t + \frac{A_B}{2R_B} \dot{z}_B \right] \end{aligned}$$

which is the final form of the radial dissipation force.

4.7 Equation Of Motion

Combining the results of the previous sections the equation of motion for the buoy is

$$\begin{aligned} \rho A_B L_B \left[1 + C_h \left(1 - \frac{z_B}{L_B} \right) \right] \ddot{z}_B &= -D_{WB} - \rho g A_B z_B \\ &\quad - \left(\frac{2\rho\omega A_B}{k^2 R_B} \sin^2kR_B \right) e^{-k(L_B - z_B)} \dot{z}_B \end{aligned}$$

$$\begin{aligned}
& + \frac{1}{2^p} (-2\dot{z}_B I_2 + A_B \dot{z}_B^2) (C_D \operatorname{sgn} v) + \frac{1}{2^p} I_1 (C_D \operatorname{sgn} v) + p_{aB} A_B \\
& + \frac{\pi \rho g H}{k} e^{-k(L_B - z_B)} \left[R_B J_1(kR_B) - R_W J_1(kR_W) \right] \left[1 - C_h k(L_B - z_B) \right] \cos \omega t \\
& - \left[\frac{4\rho \omega^2 H}{k^3} e^{-3k(L_B - z_B)} \sin^2 kR_B \sin \frac{kA_B}{4R_B} \right] \sin \omega t \quad (4-1)
\end{aligned}$$

where

$$I_1 = \frac{1}{2} \left[\frac{\omega H}{2k} e^{-k(L_B - z_B)} \right]^2 \left\{ A_B - \frac{\pi}{k} \left[R_B J_1(kR_B) - R_W J_1(kR_W) \right] \cos 2\omega t \right\} \quad (4-2)$$

$$I_2 = - \frac{\pi \omega H}{k} e^{-k(L_B - z_B)} \left[R_B J_1(kR_B) - R_W J_1(kR_W) \right] \sin \omega t \quad (4-3)$$

$$D_{WB} = \frac{\pi}{4^p} f R_W (L_W + z_W - z_B) (\dot{z}_B - \dot{z}_W) \left| (\dot{z}_B - \dot{z}_W) \right| \quad (4-4)$$

$$\operatorname{sgn} v = \left| - \frac{\pi \omega H}{k A_B} e^{-k(L_B - z_B)} \left[R_B J_1(kR_B) - R_W J_1(kR_W) \right] \sin \omega t - \dot{z}_B \right| \quad (4-5)$$

The air pressure force on the buoy, $p_{aB} A_B$, is developed in the next chapter.

5. AIR COLUMN ANALYSIS

5.1 Introduction

The motion of the air above the water column free surface is analyzed in order to determine the mass flow delivered to the turbine and the pressure forces acting on the water column and buoy. The question arises as to just how to treat this air flow; compressible or incompressible, viscous or non-viscous, steady or unsteady? The assumptions made are that the flow is incompressible, non-viscous, and steady. These assumptions are justified by the arguments to follow.

The air at the water/air interface has velocity

$$\dot{z}_A = \dot{z}_W - \dot{z}_B$$

and this velocity will rarely, if ever, exceed a few feet per second for the buoy systems and deployments of interest. Throughout the air passage, which is shown in Figure 5-1, compressibility effects can certainly be neglected. The turbine nozzle areas are such that the air velocity will increase by a factor of about 150 and so even at the nozzle exits the velocity will rarely exceed several hundred feet per second and compressibility effects can again be neglected.

The fluid can be treated as non-viscous but in computing pressures various head losses can be included. With these assumptions, the Bernoulli equation along any streamline is

$$\int_1^2 \frac{\partial V}{\partial t} ds + \frac{V_2^2}{2} + \frac{p_2}{\rho} + gz_2 = \frac{V_1^2}{2} + \frac{p_1}{\rho} + gz_1$$

and for the moment consider a straight passage from the internal free surface to the turbine nozzles. Since the continuity equation applies, $\partial V/\partial t$ is not a function of s , the distance along the passage, so

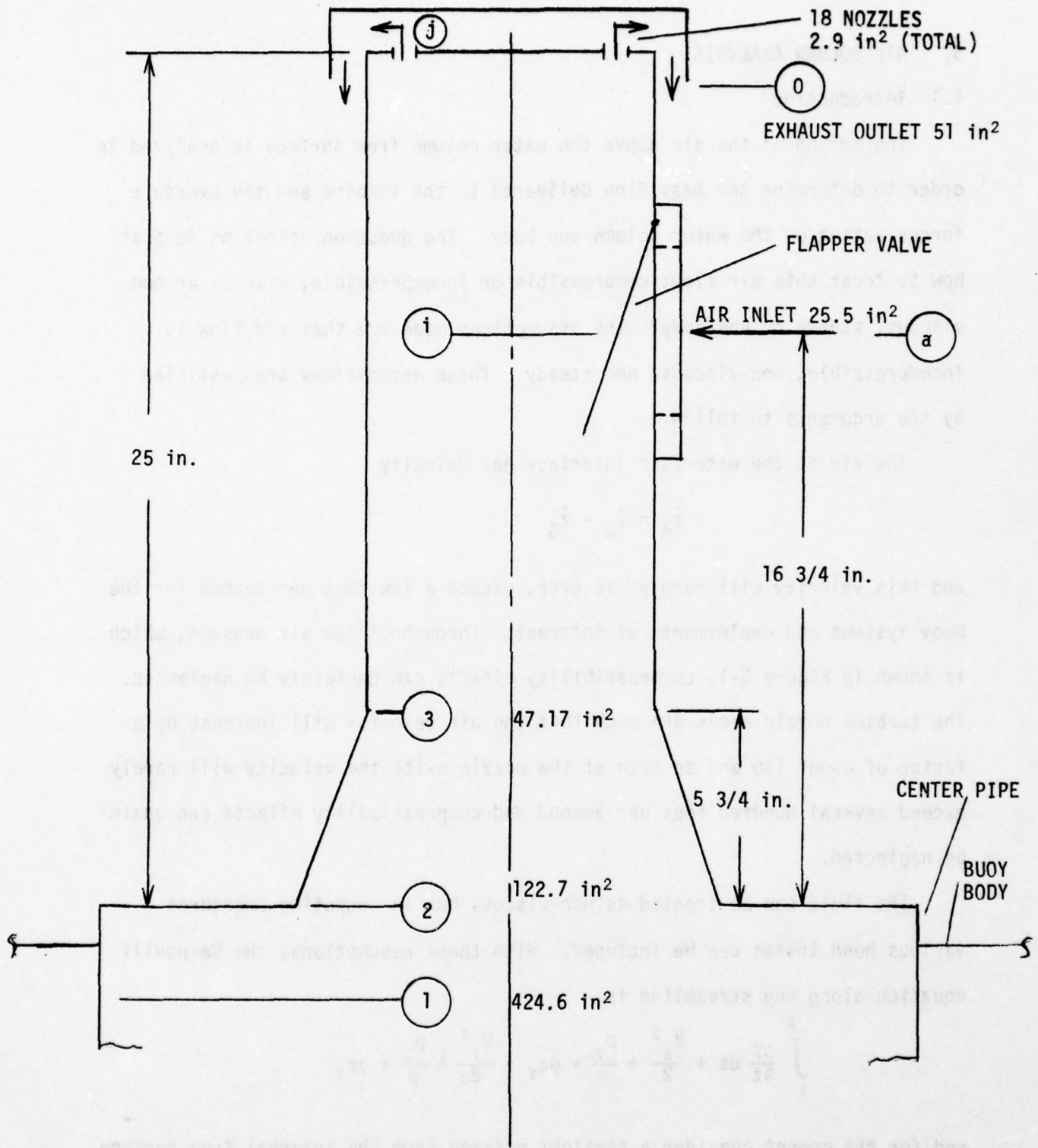


FIGURE 5-1. WATG-4 INTERNAL AIR PASSAGE CONFIGURATION

$$\dot{V}(z_2 - z_1) + \frac{V_j^2}{2} + \frac{p_j}{\rho} + g(z_2 - z_1) = \frac{V_1^2}{2} + \frac{p_1}{\rho}$$

Now, assuming the nozzles exhaust to atmosphere and applying the continuity equation

$$VA_w = V_j A_j$$

$$\frac{p_1}{\rho} = (\dot{V} + g)(z_2 - z_1) + \frac{V^2}{2} \left[\left(\frac{A_w}{A_j} \right)^2 - 1 \right]$$

where

$$V = \dot{z}_w - \dot{z}_B$$

Now assume a steady-state response to a sinusoidal wave input so that

$$V = A\Omega \sin\Omega t$$

$$\dot{V} = A\Omega^2 \cos\Omega t$$

so

$$\frac{p_1}{\rho} = (A\Omega^2 \cos\Omega t + g) L_a + \frac{A^2\Omega^2}{2} \left[\left(\frac{A_w}{A_j} \right)^2 - 1 \right] \sin^2\Omega t$$

where

$A\Omega$ = magnitude of air velocity

L_a = length of air passage

approximate values are

$$L_a = 3 \text{ feet}$$

$$\left(\frac{A_w}{A_j} \right)^2 - 1 = 21400$$

so

$$\frac{p_1}{\rho} = 3(A\Omega^2 \cos\Omega t + g) + 10720(A\Omega)^2 \sin^2\Omega t$$

For a typical air motion values might be

$$A\Omega = 4 \text{ FPS}$$

$$\Omega = \pi \text{ RAD/SEC}$$

so

$$\frac{p_1}{\rho} \sim 100 + 40 \cos\Omega t + 160000 \sin^2\Omega t$$

so that the only time at which the unsteady and gravity terms have an appreciable effect is in the vicinity of $\Omega t = 0$ and 180° , and at these times the pressure is small (on the order of 1/4 PSF). As far as the pressure forces are concerned, then, these terms can be neglected. These terms will have an effect on the time at which the intake valve opens or closes ($p_1 = 0$) but the precise timing of this event is not considered significant. In fact, the valve is a simple flapper of very low inertia and it will be assumed that when

$$\dot{z}_A > 0 \quad \text{valve is closed}$$

$$\dot{z}_A < 0 \quad \text{valve is opened}$$

With these assumptions, then, the air velocity delivered to the turbine is

$$V_j = \frac{A_w}{A_j} \dot{z}_A \quad \text{for } \dot{z}_A > 0 \quad (5-1)$$

$$V_j = 0 \quad \text{for } \dot{z}_A < 0 \quad (5-2)$$

The air pressure forces can now be determined by the application of the steady form of the Bernoulli equation.

5.2 Intake Valve Closed ($\dot{z}_A > 0$)

In the analysis that follows the symbols used are

$$p = \text{air pressure} \quad \rho = \text{air density}$$

$$V = \text{air velocity} \quad h = \text{loss coefficient}$$

and the subscripts refer to stations in the air passage which are identified in Figure 5-1.

5.2.1. Station 1 to 2

$$\frac{p_2}{\rho} + \frac{V_2^2}{2} (1 + h_{12}) = \frac{p_1}{\rho} + \frac{V_1^2}{2}$$

$$V_2 A_2 = V_1 A_1$$

$$p_1 - p_2 = \frac{\rho V_1^2}{2} \left[(1 + h_{12}) \left(\frac{A_1}{A_2} \right)^2 - 1 \right]$$

h_{12} = loss coefficient for a sudden contraction

5.2.2. Station 2 to 3

$$\frac{p_3}{\rho} + \frac{V_3^2}{2} (1 + h_{23}) = \frac{p_2}{\rho} + \frac{V_2^2}{2}$$

$$A_3 V_3 = A_2 V_2 = A_1 V_1$$

$$p_2 - p_3 = \frac{\rho V_1^2}{2} \left[(1 + h_{23}) \left(\frac{A_1}{A_3} \right)^2 - \left(\frac{A_1}{A_2} \right)^2 \right]$$

h_{23} = loss coefficient for a convergent section

5.2.3. Station 3 to i

There is no area change in this section and if friction at the wall is neglected

$$p_3 = p_i$$

5.2.4. Station i to j

$$\frac{p_j}{\rho} + \frac{V_j^2}{2} (1 + h_{sj}) = \frac{p_i}{\rho} + \frac{V_i^2}{2}$$

$$A_j V_j = A_3 V_3 = A_2 V_2 = A_1 V_1$$

$$p_3 - p_j = \frac{\rho V_1^2}{2} \left[(1 + h_{3j}) \left(\frac{A_1}{A_j} \right)^2 - \left(\frac{A_1}{A_3} \right)^2 \right]$$

h_{3j} = nozzle loss coefficient

5.2.5. Air pressures

Assuming that the nozzles exhaust to atmosphere, and since $V_1 = \dot{z}_A$ and $A_1 = A_W$ the final pressures are

$$p_1 = \frac{\rho \dot{z}_A^2}{2} \left[\left(\frac{A_W}{A_j} \right)^2 - 1 + h_{12} \left(\frac{A_W}{A_2} \right)^2 + h_{23} \left(\frac{A_W}{A_3} \right)^2 + h_{3j} \left(\frac{A_W}{A_j} \right)^2 \right]$$

$$p_2 = \frac{\rho \dot{z}_A^2}{2} \left[\left(\frac{A_W}{A_j} \right)^2 - \left(\frac{A_W}{A_2} \right)^2 + h_{23} \left(\frac{A_W}{A_3} \right)^2 + h_{3j} \left(\frac{A_W}{A_j} \right)^2 \right]$$

$$p_3 = p_j = \frac{\rho \dot{z}_A^2}{2} \left[\left(\frac{A_W}{A_j} \right)^2 - \left(\frac{A_W}{A_3} \right)^2 + h_{3j} \left(\frac{A_W}{A_j} \right)^2 \right]$$

5.2.6. Force on water column

The air pressure force on the water column acts down (-) during this phase ($\dot{z}_A > 0$) and is

$$F_w = - p_{aw} A_w = - p_1 A_w$$

$$p_{aw} A_w = A_w \frac{\rho \dot{z}_A^2}{2} \left[\left(\frac{A_W}{A_j} \right)^2 - 1 + h_{12} \left(\frac{A_W}{A_2} \right)^2 + h_{23} \left(\frac{A_W}{A_3} \right)^2 + h_{3j} \left(\frac{A_W}{A_j} \right)^2 \right] \quad (5-3)$$

This is the air pressure force required in Equation (3-1).

5.2.7. Force on the buoy

The air pressure force on the buoy acts up (+) during this phase ($\dot{z}_A > 0$) and is

$$F_B = p_{aB} A_B = p_2 (A_W - A_2) + p_3 (A_3 - A_j) + \bar{p}_{23} (A_2 - A_3) + F_M$$

where \bar{p}_{23} is the area-averaged pressure in the short convergent section between stations 2 and 3 and F_M is the force due to the turning of the air stream 180° as it is exhausted from the annular outlet of area A_0 . It can be shown that

$$\bar{p}_{23} = p_2 + \frac{\rho \dot{z}_A^2}{2} \left(\frac{A_W}{A_2} \right)^2 \left(1 - \frac{A_2}{A_3} \right)$$

$$F_M = \rho A_W \dot{z}_A^2 \left(1 + \frac{A_W}{A_0} \right)$$

so

$$p_{aB} A_B = A_B \frac{\rho \dot{z}_A^2}{2} \left\{ \left(\frac{A_W}{A_j} \right)^2 (1 + h_{3j}) \left(\frac{A_W - A_j}{A_B} \right) - \left(\frac{A_W}{A_2} \right)^2 \left[\frac{A_W + \left(\frac{A_2}{A_3} - 2 \right) A_2}{A_B} \right] \right. \\ \left. + \left(\frac{A_W}{A_3} \right)^2 \left[\frac{h_{23} A_W - (1 + h_{23}) A_3 + A_j}{A_B} \right] + 2 \left(1 + \frac{A_W}{A_0} \right) \left(\frac{A_W}{A_B} \right) \right\} \quad (5-4)$$

This is the air pressure force required in Equation (4-1).

5.3 Intake Valve Open ($\dot{z}_A < 0$)

A similar analysis is made for the intake flow when the valve is open.

5.3.1. Station a to i

If the velocity on the atmospheric side of the intake valve is assumed to be zero

$$\frac{p_i}{\rho} + \frac{V_i^2}{2} (1 + h_{ai}) = \frac{p_a}{\rho}$$

$$A_i V_i = A_1 V_1$$

$$p_i - p_a = - \frac{\rho V_1^2}{2} (1 + h_{ai}) \left(\frac{A_1}{A_i} \right)^2$$

h_{ai} = loss coefficient for the inlet port

5.3.2. Station i to 3

$$p_3 - p_i = \frac{\rho V_1^2}{2} \left[\left(\frac{A_1}{A_i} \right)^2 - \left(\frac{A_1}{A_3} \right)^2 \right]$$

5.3.3. Station 3 to 2

$$p_2 - p_3 = \frac{\rho V_1^2}{2} \left[\left(\frac{A_1}{A_3} \right)^2 - (1 + h_{32}) \left(\frac{A_1}{A_2} \right)^2 \right]$$

h_{32} = loss coefficient for a diverging section

5.3.4. Station 2 to 1

$$p_1 - p_2 = \frac{\rho V_1^2}{2} \left[\left(\frac{A_1}{A_2} \right)^2 - (1 + h_{21}) \right]$$

h_{21} = loss coefficient for a sudden enlargement

5.3.5. Air pressures

Assuming that p_a is atmospheric, the final pressures are

$$p_1 = - \frac{\rho \dot{z}_a^2}{2} \left[1 + h_{21} + h_{32} \left(\frac{A_w}{A_2} \right)^2 + h_{ai} \left(\frac{A_w}{A_i} \right)^2 \right]$$

$$p_2 = - \frac{\rho \dot{z}_a^2}{2} \left[\left(\frac{A_w}{A_2} \right)^2 (1 + h_{32}) + h_{ai} \left(\frac{A_w}{A_i} \right)^2 \right]$$

$$p_3 = - \frac{\rho \dot{z}_a^2}{2} \left[\left(\frac{A_w}{A_3} \right)^2 + h_{ai} \left(\frac{A_w}{A_i} \right)^2 \right]$$

$$p_i = - \frac{\rho \dot{z}_a^2}{2} (1 + h_{ai}) \left(\frac{A_w}{A_i} \right)^2$$

5.3.6. Force on water column

The air pressure force on the water column acts up (+) during this

phase ($\dot{z}_A < 0$) and is

$$F_w = p_{aw}A_w = p_1A_1 = -A_w \frac{\rho \dot{z}_a^2}{2} \left[1 + h_{21} + h_{32} \left(\frac{A_w}{A_2} \right)^2 + h_{a1} \left(\frac{A_w}{A_1} \right)^2 \right] \quad (5-5)$$

This is the air pressure force required in Equation (3-1).

5.3.7. Force on the buoy

The air pressure force on the buoy acts down (-) during this phase ($\dot{z}_A < 0$) and is

$$F_B = p_{aB}A_B = p_2(A_1 - A_2) + \bar{p}_{23}(A_2 - A_3) + p_1A_3$$

where \bar{p}_{23} is the area-averaged pressure in the short divergent section between stations 3 and 2. It can be shown that

$$\bar{p}_{23} = p_3 + \frac{\rho V_1^2}{2} \left(\frac{A_1}{A_3} \right)^2 \left(1 + \frac{A_3}{A_2} \right)$$

so

$$p_{aB}A_B = -A_B \frac{\rho \dot{z}_a^2}{2} \left[\left(\frac{A_w}{A_2} \right)^2 (1 + h_{32}) \left(\frac{A_w - A_2}{A_B} \right) + \left(\frac{A_w}{A_1} \right)^2 \left(\frac{h_{a1}A_w + A_3}{A_B} \right) - \left(\frac{A_w}{A_3} \right) \left(\frac{A_w}{A_2} \right) \left(\frac{A_2 - A_3}{A_B} \right) \right] \quad (5-6)$$

This is the air pressure force required in Equation (4-1).

6. TURBINE TORQUE

6.1 Basic Theory

Basic reaction turbine theory from Reference 8, Chapter 5 is presented in order to analyze the air flow over the turbine blades so that the torque produced can be related to turbine geometry and buoy system variables. The configuration of the velocity vectors is shown in Figure 6-1. The symbols are defined as follows:

V_j = velocity of the air exiting the nozzles

U = relative air velocity due to turbine rotation

V_1 = net entering air velocity

V_2 = net exiting air velocity

V_m = mean air velocity

α_j = nozzle angle

α_1 = entering angle of flow

β_2 = exiting angle of flow

α_m = mean angle of attack

F_t = tangential force on a blade due to lift and drag

From Reference 8

$$F_t = \frac{\rho V_m^2}{2} A_b (C_L \cos \alpha_m \pm C_D \sin \alpha_m)$$

A_b = blade area = span x chord = bc

Reference 8 states that for well-designed blades the drag terms are generally negligible so this will be assumed. The lift coefficient can be approximated as

$$C_L = 2\pi K \sin \alpha_m$$

where K is the cascade coefficient and depends upon the outlet angle, β_2 , and the blade pitch-to-chord ratio (s/c). Substituting

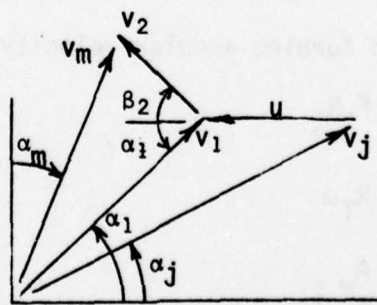
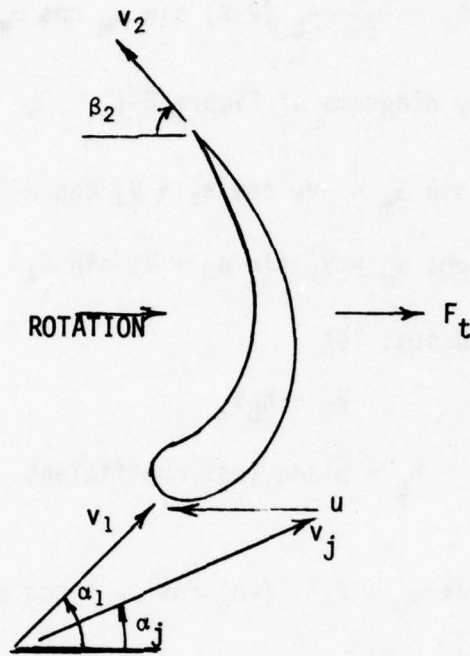


FIGURE 6-1. TURBINE BLADE VELOCITY DIAGRAMS

$$F_t = \frac{\rho V_m^2}{2} A_b (2\pi K) \sin \alpha_m \cos \alpha_m$$

Now, from the velocity diagrams of Figure 6-1

$$V_m \sin \alpha_m = -V_2 \cos \beta_2 + V_1 \cos \alpha_1$$

$$V_m \cos \alpha_m = V_2 \sin \beta_2 + V_1 \sin \alpha_1$$

and, to account for losses, let

$$V_2 = h_b V_1$$

h_b = blade loss coefficient

so that

$$V_m^2 \sin \alpha_m \cos \alpha_m = V_1^2 (-h_b \cos \beta_2 + \cos \alpha_1) (h_b \sin \beta_2 + \sin \alpha_1)$$

Also, from the velocity diagrams

$$V_1^2 = V_j^2 + U^2 - 2V_j U \cos \alpha_j \quad (6-1)$$

$$\cos \alpha_1 = \frac{V_j \cos \alpha_j - U}{V_1}, \quad \sin \alpha_1 = \frac{V_j \sin \alpha_j}{V_1} \quad (6-2)$$

and

$$F_t = \pi \rho K A_b V_1^2 (-h_b \cos \beta_2 + \cos \alpha_1) (h_b \sin \beta_2 + \sin \alpha_1) \quad (6-3)$$

Equations (6-1), (6-2), (6-3) allow the turbine torque to be found as a function of air velocity and turbine angular velocity since

$$T = F_t R_T$$

$$U = R_T \omega$$

$$V_j = \frac{A_w}{A_j} \dot{z}_a$$

where R_T is the turbine radius. From an analog simulation standpoint, these equations could be solved but would require seven multipliers. Since these equations are not precise, it seems desirable to take an approach that would require fewer multipliers but still preserve the essentials of the torque variation.

6.2 Simplified Torque Analysis

For an ideal impulse turbine the torque - speed variation is linear with maximum torque at zero speed and zero torque at an RPM corresponding to blade stall. Reference 8 states that a well-designed reaction turbine approximates this behavior. This approximation will be employed.

If the turbine has n blades, then at zero RPM $U = 0$ and Equations (6-1), (6-2), (6-3) can be reduced to give the total torque T_0 as

$$T_0 = C_T V_j^2$$

$$C_T = n \pi \rho K A_b R_T (-h_b \cos \beta_2 + \cos \alpha_j) (h_b \sin \beta_2 + \sin \alpha_j)$$

and, employing the linear approximation

$$T = T_0 - m \omega$$

where m is to be found.

From Equation (6-3) the torque is zero when

$$\cos \alpha_1 = h_b \cos \beta_2 = \frac{V_j \cos \alpha_j - U_0}{V_1}$$

so, using Equation (6-1)

$$(V_j^2 + U_0^2 - 2V_j U_0 \cos \alpha_j) (h_b \cos \beta_2)^2 = V_j^2 \cos^2 \alpha_j - 2V_j U_0 \cos \alpha_j + U_0^2$$

or

$$U_0^2 - (2V_j \cos \alpha_j) U_0 + V_j^2 \frac{\cos^2 \alpha_j - (h_b \cos \beta_2)^2}{1 - (h_b \cos \beta_2)^2} = 0$$

and solving this quadratic

$$\frac{U_o}{V_j \cos \alpha_j} = 1 \pm (\tan \alpha_j) \sqrt{\frac{(h_b \cos \beta_2)^2}{1 - (h_b \cos \beta_2)^2}}$$

Using the minus sign, the lowest speed at which the torque goes to zero is

$$U_o = k V_j \cos \alpha_j$$

$$k = 1 - (\tan \alpha_j) \sqrt{\frac{(h_b \cos \beta_2)^2}{1 - (h_b \cos \beta_2)^2}}$$

and since

$$T = T_o - m\omega$$

$$m = T_o / w_o = \frac{T_o R_T}{U_o}$$

so

$$T = T_o - \frac{T_o R_T}{U_o} \omega$$

$$= T_o \left(1 - \frac{R_T \omega}{k V_j \cos \alpha_j} \right)$$

$$= C_T V_j^2 \left(1 - \frac{R_T \omega}{k V_j \cos \alpha_j} \right)$$

$$= C_T V_j \left(V_j - \frac{R_T \omega}{k \cos \alpha_j} \right)$$

or

$$T = C_T V_j (V_j - C_s \omega) \tag{6-4}$$

$$C_s = R_T / k \cos \alpha_j \tag{6-5}$$

$$k = 1 - (\tan \alpha_j) \sqrt{\frac{(h_b \cos \beta_2)^2}{1 - (h_b \cos \beta_2)^2}} \quad (6-6)$$

$$C_T = n\pi\rho K A_b R_T (-h_b \cos \beta_2 + \cos \alpha_j) (h_b \sin \beta_2 + \sin \alpha_j) \quad (6-7)$$

$$v_j = \left(\frac{A_w}{A_j} \right) \dot{z}_A \quad \text{for } \dot{z}_A > 0 \quad (6-8)$$

$$v_j = 0 \quad \text{for } \dot{z}_A < 0 \quad (6-9)$$

This set of equations gives the input torque to the turbine/generator system as a function of the buoy/water column motion.

7. TURBINE/GENERATOR EQUATIONS

7.1 Generator Characteristics

The WATG employs a 3-phase alternator to generate an a.c. signal which is rectified and supplies current to charge a 12-volt battery. If the battery is fully charged a control circuit diverts the current to a resistor where it is dissipated. The no-load voltage and charging current into a 12-volt load are shown in Figure 7-1 as a function of generator RPM. The generator is directly coupled to the turbine so generator and turbine RPM are the same. The detailed analysis of the electromechanical equations is quite complex but does not appear to be necessary for this study since only two questions need be answered: First, given the turbine angular velocity what is the current generated? Second, given the input torque due to air flow what is the turbine angular velocity? The first question is answered by using the generator characteristic shown in Figure 7-1. For the analog simulation, this curve is duplicated using a variable diode function generator. The second question is answered by analyzing the turbine/generator dynamics using a simplified equation of motion which includes an electromagnetic torque proportional to the current generated. The equation of motion is developed in the next section.

7.2 Turbine/Generator Equation of Motion

The equation of motion is developed from the relation

$$J\dot{\omega} = \text{sum of torques}$$

$$J = \text{mass moment of inertia of turbine rotor and generator rotor}$$

The torques applied consist of

$$T = \text{Torque due to air flow over the turbine blades (given by Equation (6-4))}$$

$$T_D = \text{torque due to friction and windage losses}$$

$$T_E = \text{torque due to current generated}$$

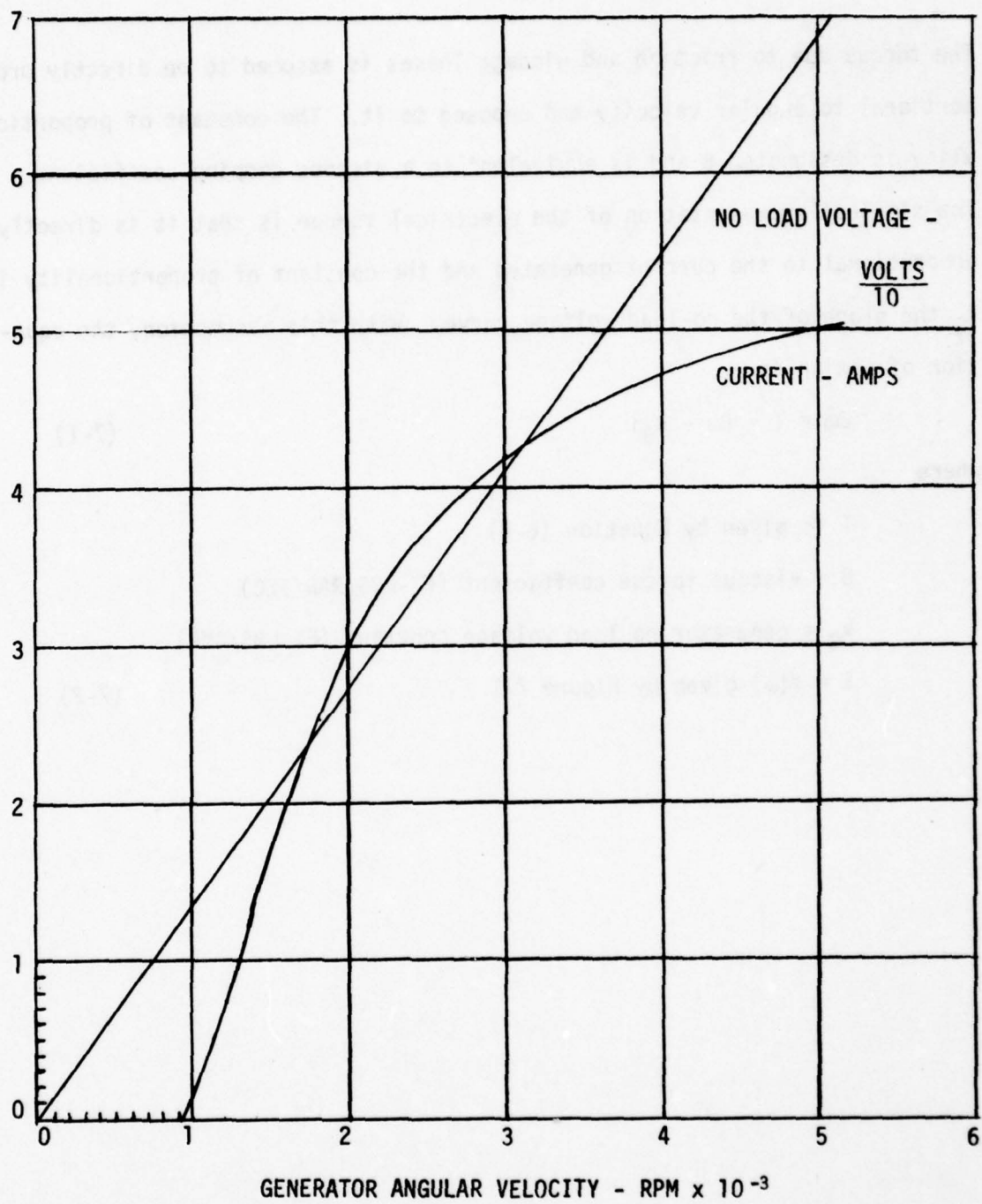


FIGURE 7-1. WATG-4 ALTERNATOR INPUT-OUTPUT CHARACTERISTICS

The torque due to friction and windage losses is assumed to be directly proportional to angular velocity and opposed to it. The constant of proportionality is designated B and is equivalent to a viscous damping coefficient. The simplest representation of the electrical torque is that it is directly proportional to the current generated and the constant of proportionality is k_G the slope of the no-load voltage curve. With this assumption, the equation of motion is

$$J\dot{\omega} = T - B\omega - k_G i \quad (7-1)$$

where

T is given by Equation (6-4)

B = viscous torque coefficient (FT-LBS/RAD/SEC)

k_G = generator no-load voltage constant (FT-LBS/AMP)

$i = f(\omega)$ given by Figure 7-1 (7-2)

8. ANALOG SIMULATION

8.1 Introduction

The equations necessary to simulate the WATG have been developed in the preceding chapters and are identified as follows:

<u>ELEMENT</u>	<u>EQUATION NUMBERS</u>
Water Column Dynamics	(3-1)
Buoy Dynamics	(4-1) through (4-5)
Air Pressure Forces	(5-1) through (5-6)
Turbine Torque	(6-4) through (6-7)
Turbine/Generator Dynamics	(7-1) and (7-2)

The scaled computer equations and the analog patching diagrams are developed in this chapter. The symbols used in the diagrams are shown in Table 8-1.

8.2 Wave Forcing Functions

An examination of equations (3-1) and (4-1) through (4-5) shows that wave forcing functions proportional to $\sin\Omega t$, $\cos\Omega t$, and $\cos 2\Omega t$ are required. The generation of unit amplitude sinusoidal functions is a standard analog technique and the required patching diagrams are shown in Figure 8-1. The characteristics of the input wave are shown in Table 8-2 where

T = wave period

$\Omega = 2\pi/T$ = wave frequency

$\lambda = \frac{gT^2}{2\pi}$ = wavelength

$k = 2\pi/\lambda$ = wave number

$$C_{\eta} = \frac{2\pi}{k^2 A_B} e^{-kL_B} [kR_B J_1(kR_B) - kR_W J_1(kR_W)]$$

and $\frac{H}{2} C_{\eta}$ is the amplitude of the wave at a depth equal to the buoy draft L_B .

Table 8-1. ANALOG SYMBOLS

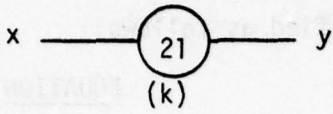
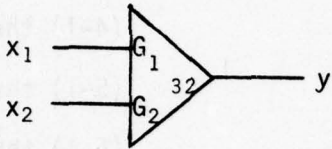
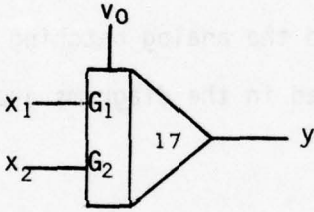
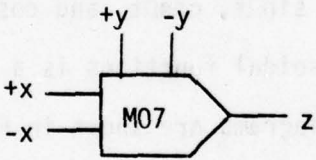
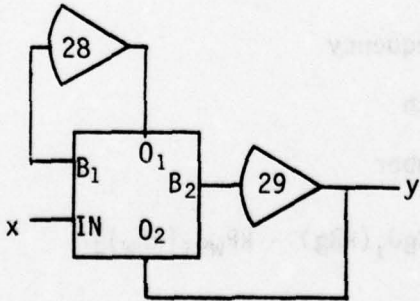
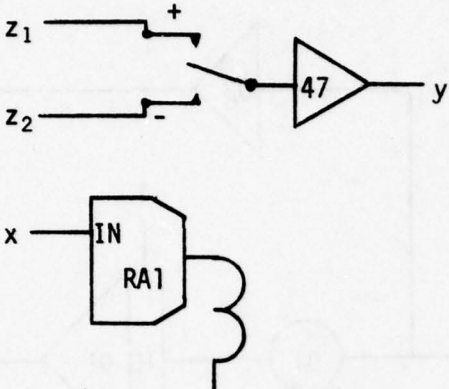
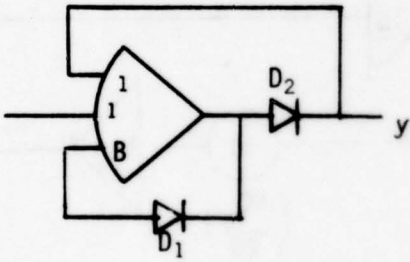
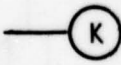
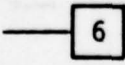
ELEMENT	SYMBOL	EQUATION
Potentiometer		$y = kx$
Summer		$y = - (G_1x_1 + G_2x_2)$
Integrator		$y = -V_0 - \int_0^t (G_1x_1 + G_2x_2)dt$
Multiplier		$z = -xy$
Variable Diode Function Generator		$y = f(x)$

Table 8-1. CONTINUED

ELEMENT	SYMBOL	EQUATION
Relay Comparator		<p>If $x > 0$ $y = z_1$</p> <p>If $x < 0$ $y = z_2$</p>
Zero Limiter		<p>If $x > 0$ $y = -x$</p> <p>If $x < 0$ $y = 0$</p>
Interconnection		Shows connections among various circuits
Output		Shows recorder channel number

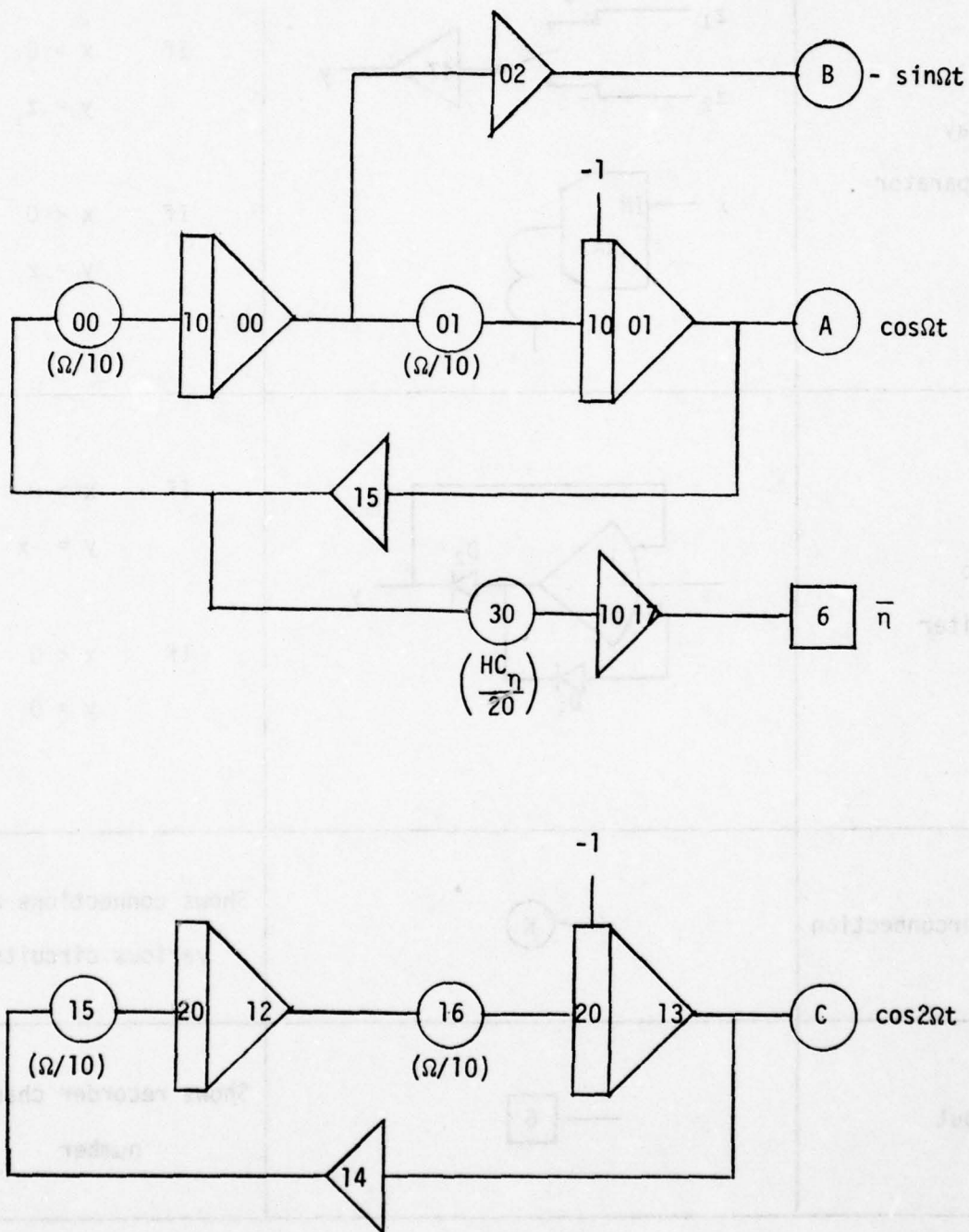


Figure 8-1. SINUSOIDAL WAVE INPUT FUNCTIONS

Table 8-2. WAVE EXCITATION PARAMETERS

Period T (sec)	Frequency Ω (rad/sec)	Wavelength λ (ft)	Wave Number k (ft ⁻¹)	Amplitude Coefficient C_n
1.0	6.283	5.125	1.226	-0.0014
1.2	5.236	7.380	0.8514	0.0016
1.4	4.488	10.04	0.6255	0.0295
1.6	3.927	13.12	0.4789	0.0857
1.8	3.491	16.60	0.3784	0.1592
2.0	3.142	20.50	0.3065	0.2384
2.2	2.856	24.80	0.2533	0.3156
2.4	2.618	29.52	0.2128	0.3869
2.6	2.417	34.64	0.1814	0.4510
2.8	2.244	40.18	0.1564	0.5076
3.0	2.094	46.12	0.1362	0.5573
3.2	1.963	52.48	0.1197	0.6008
3.4	1.848	59.24	0.1060	0.6387
3.6	1.745	66.42	0.0946	0.6720
3.8	1.653	74.00	0.0849	0.7012
4.0	1.571	82.00	0.0766	0.7269
4.2	1.496	90.40	0.0695	0.7495
4.4	1.428	99.22	0.0633	0.7696
4.6	1.366	108.4	0.0579	0.7875
4.8	1.309	118.1	0.0532	0.8034
5.0	1.257	128.1	0.0490	0.8177
5.2	1.208	138.6	0.0453	0.8305
5.4	1.164	149.4	0.0420	0.8420
5.6	1.122	160.7	0.0391	0.8524
5.8	1.083	172.4	0.0364	0.8619
6.0	1.047	184.5	0.0340	0.8705

The values used are for an 8 x 26 buoy

$$R_B = 4 \text{ feet}$$

$$R_W = 1 \text{ foot}$$

$$A_B = \pi(R_B^2 - R_W^2) = 15\pi \text{ ft}^2$$

$$L_B = 4 \text{ feet}$$

8.3 Water Column Dynamics

For simulation purposes equation (3-1) is simplified by assuming that the vertical motions of the buoy and water column are small compared to the water column length. Dividing through by $\rho A_W L_W$ and letting the scaling factors be denoted by

A = acceleration scale factor

V = velocity scale factor

δ = displacement scale factor

The scaled equation is

$$\left[\frac{\ddot{z}_W}{A} \right] = -C_{W\delta} \left[\frac{z_W}{\delta} \right] + C_{Wf} \left[\frac{\dot{z}_B}{V} - \frac{\dot{z}_W}{V} \right] \left[\left| \frac{\dot{z}_B}{V} - \frac{\dot{z}_W}{V} \right| \right] - \frac{P_{aw}}{\rho L_W A} + \bar{H}_W \cos \Omega t$$

where

$$\bar{H}_W = \frac{H}{A} \frac{g J_1(k R_W)}{R_W} \frac{e^{-k L_W}}{k L_W}$$

$$C_{W\delta} = \frac{g \delta_W}{A L_W}$$

$$C_{Wf} = \frac{f V^2}{4 R_W A}$$

for

$$R_W = 1 \text{ foot}$$

$$f = 0.020$$

$$\frac{A\bar{H}_W}{H} = 32.2 J_1(k) \frac{e^{-kL_W}}{kL_W} (\text{sec}^{-2})$$

$$\frac{AC_{W\delta}}{\delta} = \frac{32.2}{L_W} (\text{sec}^{-2})$$

$$\frac{AC_{Wf}}{V^2} = 0.005$$

Since the water column length is to be a parameter in the simulation, Table 8-3 presents these coefficients for various values of L_W . The air pressure force term is given in Section 8.5. The analog patching diagram is shown in Figure 8-2.

8.4 Buoy Dynamics

For simulation purposes, equations (4-1) through (4-5) are simplified by assuming the vertical motions of the buoy and water column are small compared to the buoy length L_B . Dividing through by $\rho A_B L_B (1 + C_h)$ and using the previously defined scaling factors, the buoy equation of motion is

$$\begin{aligned} \left[\frac{\ddot{z}_B}{A} \right] = & - C_{BV_1} \left[\frac{\dot{z}_B}{V} \right] + C_{BV_2} \left(2\bar{H}_{B1} \sin\Omega t + \left[\frac{\dot{z}_B}{V} \right] \right) \left(C_D \text{sgn} \frac{v}{V} \right) \left[\frac{\dot{z}_B}{V} \right] \\ & - C_{Bf} \left[\frac{\dot{z}_B}{V} - \frac{\dot{z}_W}{V} \right] \left[\left| \frac{\dot{z}_B}{V} - \frac{\dot{z}_W}{V} \right| \right] - C_{B\delta} \left[\frac{z_B}{\delta} \right] \\ & + C_{BH_1} \bar{H}_{B1} \cos\Omega t - C_{BH_3} \bar{H}_{B3} \sin\Omega t \\ & + C_{BH_2} \bar{H}_{B2} \left(\bar{H}_{B2} - \bar{H}_{B1} \cos 2\Omega t \right) \left(C_D \text{sgn} \frac{v}{V} \right) + \frac{P_{aB}}{\rho L_B A (1 + C_h)} \end{aligned}$$

where

$$\frac{v}{V} = \bar{H}_{B1} \sin\Omega t + \frac{\dot{z}_B}{V}$$

Table 8-3. COEFFICIENTS FOR WATER COLUMN EQUATION OF MOTION

Period, T (sec)	$L_w = 5$ ft		$L_w = 10$ ft		$L_w = 15$ ft		$L_w = 20$ ft		$L_w = 25$ ft		$L_w = 30$ ft	
	$\frac{A\bar{H}_w}{H(\text{sec}^{-2})}$	$\frac{AC_w\delta}{\delta(\text{sec}^{-2})}$	$\frac{A\bar{H}_w}{H}$	$\frac{AC_w\delta}{\delta}$	$\frac{A\bar{H}_w}{H}$	$\frac{AC_w\delta}{\delta}$	$\frac{A\bar{H}_w}{H}$	$\frac{AC_w\delta}{\delta}$	$\frac{A\bar{H}_w}{H}$	$\frac{AC_w\delta}{\delta}$	$\frac{A\bar{H}_w}{H}$	$\frac{AC_w\delta}{\delta}$
1.0	0.0058	6.440	0.0000	3.220	0.0000	2.147	0.0000	1.610	0.0000	1.288	0.0000	1.073
1.2	0.0416		0.0003		0.0000		0.0000		0.0000		0.0000	
1.4	0.1343		0.0029		0.0000		0.0000		0.0000		0.0000	
1.6	0.2854		0.0130		0.0008		0.0000		0.0000		0.0000	
1.8	0.4768		0.0359		0.0036		0.0004		0.0000		0.0000	
2.0	0.6873		0.0742		0.0107		0.0017		0.0003		0.0000	
2.2	0.9001		0.1268		0.0238		0.0050		0.0011		0.0003	
2.4	1.1046		0.1905		0.0438		0.0113		0.0031		0.0009	
2.6	1.2949		0.2614		0.0704		0.0213		0.0069		0.0023	
2.8	1.4687		0.3360		0.1025		0.0352		0.0129		0.0049	
3.0	1.6257		0.4113		0.1388		0.0527		0.0213		0.0090	
3.2	1.7664		0.4854		0.1778		0.0733		0.0322		0.0148	
3.4	1.8921		0.5567		0.2184		0.0964		0.0454		0.0222	
3.6	2.0042		0.6244		0.2594		0.1212		0.0604		0.0314	
3.8	2.1042		0.6882		0.3001		0.1472		0.0770		0.0420	
4.0	2.1935		0.7477		0.3398		0.1737		0.0948		0.0538	
4.2	2.2733		0.8030		0.3782		0.2004		0.1132		0.0667	
4.4	2.3449		0.8542		0.4149		0.2267		0.1322		0.0802	
4.6	2.4091		0.9016		0.4499		0.2525		0.1512		0.0943	
4.8	2.4669		0.9453		0.4830		0.2776		0.1702		0.1087	
5.0	2.5190		0.9856		0.5142		0.3018		0.1889		0.1232	
5.2	2.5662		1.0228		0.5436		0.3250		0.2072		0.1377	
5.4	2.6089		1.0571		0.5711		0.3471		0.2250		0.1520	
5.6	2.6478		1.0888		0.5970		0.3682		0.2423		0.1660	
5.8	2.6831		1.1181		0.6212		0.3883		0.2589		0.1798	
6.0	2.7154	6.440	1.1451	3.220	0.6439	2.147	0.4073	1.610	0.2748	1.288	0.1932	1.073

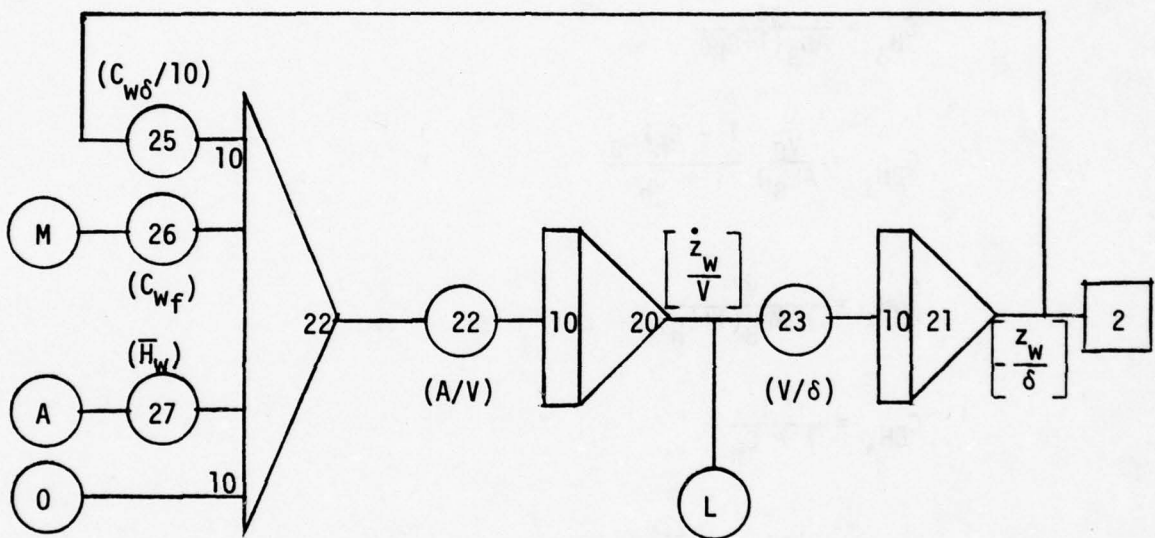


Figure 8-2. WATER COLUMN EQUATION OF MOTION

$$C_{BV_1} = \frac{2V\Omega}{A(1+C_h)} \frac{e^{-2kL_B}}{kL_B} \frac{\sin^2 kR_B}{kR_B}$$

$$C_{BV_2} = \frac{V^2}{2AL_B(1+C_h)}$$

$$C_{B_f} = \frac{\pi}{4A(1+C_h)} \frac{fV^2 R_w L_w}{A_B L_B}$$

$$C_{B_\delta} = \frac{g\delta}{AL_B(1+C_h)}$$

$$C_{BH_1} = \frac{vg}{AL_B \Omega} \frac{1 - C_h kL_B}{1 + C_h}$$

$$C_{BH_2} = \frac{V^2}{16AL_B(1+C_h)}$$

$$C_{BH_3} = \frac{1}{1 + C_h}$$

$$\bar{H}_{B_1} = H \frac{L_B}{V} \frac{\pi\Omega}{kA_B} \frac{e^{-kL_B}}{kL_B} [kR_B J_1(kR_B) - kR_w J_1(kR_w)]$$

$$\bar{H}_{B_2} = \frac{\Omega H}{V} e^{-kL_B}$$

$$\bar{H}_{B_3} = \frac{4gHk}{A} \frac{e^{-3kL_B}}{kL_B} \frac{\sin^2 kR_B \sin \frac{kA_B}{4R_B}}{k^2 A_B}$$

All parameters in the foregoing equations have been defined except C_h , which is the added mass coefficient in heave. The value of C_h is 0.65 and is derived from the experimental data discussed in Chapter 9. The coefficients which are independent of the wave parameters are

$$\frac{AC_{BV_2}}{V^2} = 0.0758 \quad \text{ft}^{-1}$$

$$\frac{AC_{Bf}}{V^2} = 5.050 \times 10^{-5} L_w \quad \text{ft}^{-1}$$

$$\frac{AC_{B\delta}}{\delta} = 4.879 \quad \text{sec}^{-2}$$

$$\frac{AC_{BH_2}}{V^2} = 0.00947 \quad \text{ft}^{-1}$$

$$C_{BH_3} = 0.6061$$

The remaining coefficients are given in Table 8-4. The air pressure force is presented in Section 8.5 and the water drag force in Section 8.6. The analog patching diagram is shown in Figure 8-3.

8.5 Air Pressure Forces

The equations describing the air pressure forces are developed in Chapter 5 and the geometry of the air passage is shown in Figure 5-1. The required scaled equations are, for $\dot{z}_w - \dot{z}_B > 0$

$$\frac{p_{aw}}{\rho AL_w} = - \frac{C_{aw} V^2}{\rho AL_w} \left(\left[\frac{\dot{z}_w}{V} \right] - \left[\frac{\dot{z}_B}{V} \right] \right)^2$$

$$\frac{p_{aB}}{\rho AL_B (1+C_h)} = \frac{C_{aB} V^2}{\rho AL_B (1+C_h)} \left(\left[\frac{\dot{z}_w}{V} \right] - \left[\frac{\dot{z}_B}{V} \right] \right)^2$$

and for $\dot{z}_w - \dot{z}_B < 0$

$$\frac{p_{aw}}{\rho AL_w} = \epsilon_w \frac{C_{aw} V^2}{\rho AL_w} \left(\left[\frac{\dot{z}_w}{V} \right] - \left[\frac{\dot{z}_B}{V} \right] \right)^2$$

Table 8-4. COEFFICIENTS FOR BUOY EQUATION OF MOTION

Period, T (sec)	$\frac{AC_{BV_1}}{V}$ (sec ⁻¹)	$\frac{AC_{BH_1}}{V}$ (sec ⁻¹)	$\frac{V\bar{H}_{B_1}}{H}$ (sec ⁻¹)	$\frac{V\bar{H}_{B_2}}{H}$ (sec ⁻¹)	$\frac{A\bar{H}_{B_3}}{H}$ (sec ⁻²)
1.0	0.0000	-1.6990	-0.0045	0.0466	0.0000
1.2	0.0000	-1.1311	0.0043	0.1738	0.0000
1.4	0.0021	-0.6811	0.0662	0.3676	0.0003
1.6	0.0249	-0.3048	0.1682	0.5782	0.0083
1.8	0.0892	0.0224	0.2780	0.7864	0.0455
2.0	0.1932	0.3152	0.3745	0.9219	0.1278
2.2	0.3200	0.5831	0.4507	1.0368	0.2490
2.4	0.4512	0.8321	0.5065	1.1174	0.3892
2.6	0.5742	1.0668	0.5449	1.1699	0.5282
2.8	0.6820	1.2901	0.5696	1.2005	0.6519
3.0	0.7725	1.5043	0.5836	1.2146	0.7534
3.2	0.8455	1.7112	0.5898	1.2163	0.8309
3.4	0.9027	1.9120	0.5902	1.2091	0.8858
3.6	0.9460	2.1078	0.5864	1.1955	0.9210
3.8	0.9777	2.2992	0.5797	1.1773	0.9396
4.0	0.9995	2.4871	0.5709	1.1561	0.9452
4.2	1.0134	2.6719	0.5606	1.1329	0.9405
4.4	1.0208	2.8540	0.5495	1.1084	0.9280
4.6	1.0230	3.0338	0.5378	1.0834	0.9098
4.8	1.0210	3.2115	0.5258	1.0580	0.8875
5.0	1.0158	3.3874	0.5138	1.0328	0.8624
5.2	1.0079	3.5617	0.5017	1.0079	0.8355
5.4	0.9980	3.7347	0.4899	0.9834	0.8076
5.6	0.9866	3.9063	0.4782	0.9596	0.7793
5.8	0.9741	4.0769	0.4668	0.9364	0.7509
6.0	0.9606	4.2464	0.4558	0.9138	0.7229

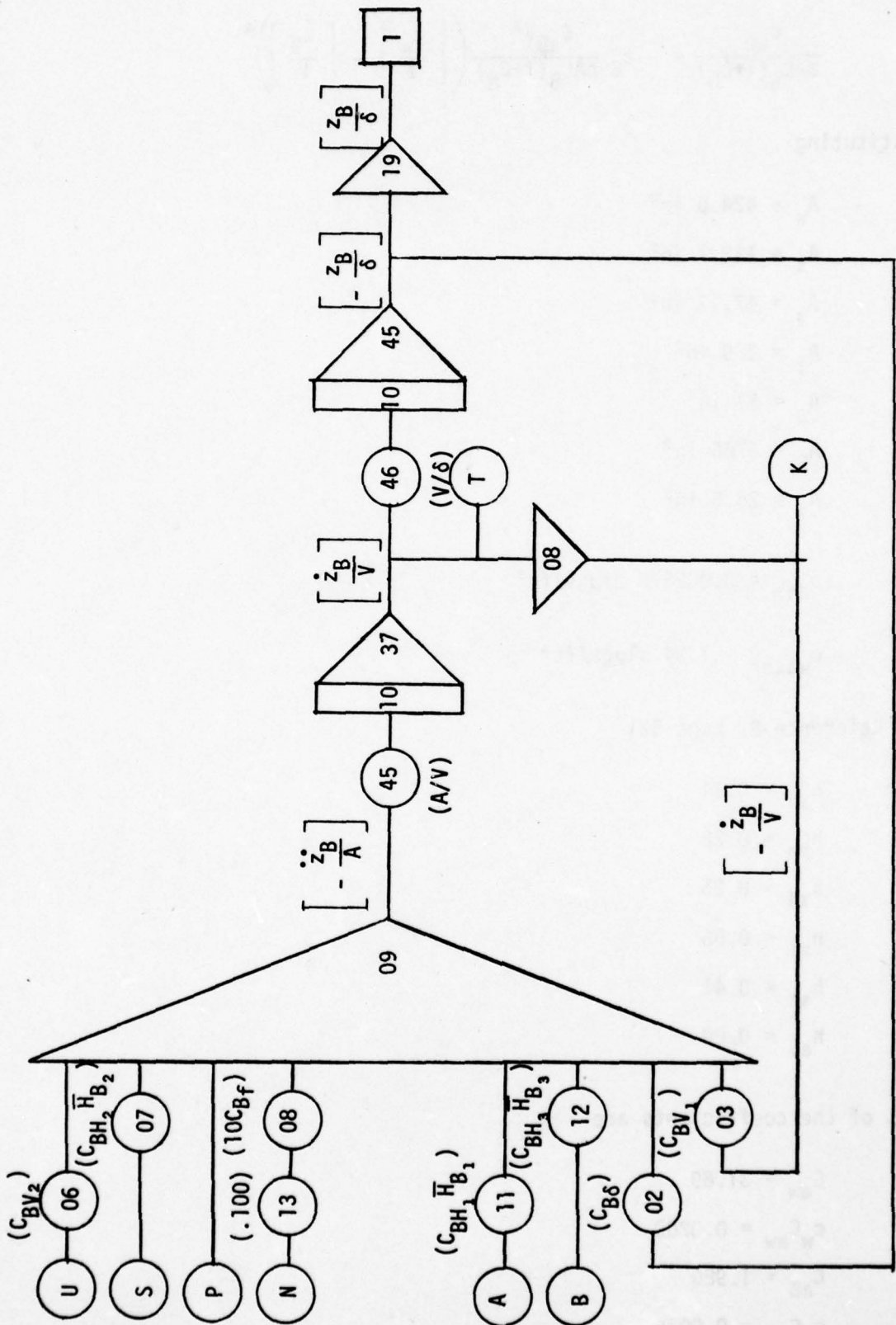


Figure 8-3. BUOY EQUATION OF MOTION

$$\frac{P_{aB}}{\rho A L_B (1+C_h)} = - \epsilon_B \frac{C_{aB} V^2}{\rho A L_B (1+C_h)} \left(\left[\frac{\dot{z}_W}{V} \right] - \left[\frac{\dot{z}_B}{V} \right] \right)^2$$

Now, substituting

$$A_w = 424.6 \text{ in}^2$$

$$A_2 = 122.7 \text{ in}^2$$

$$A_3 = 47.17 \text{ in}^2$$

$$A_j = 2.9 \text{ in}^2$$

$$A_o = 51 \text{ in}^2$$

$$A_B = 6786 \text{ in}^2$$

$$A_i = 25.5 \text{ in}^2$$

$$\rho_{\text{air}} = 0.002378 \text{ slugs/ft}^3$$

$$\rho_{\text{water}} = 1.94 \text{ slugs/ft}^3$$

and, from Reference 9, page 521

$$h_{12} = 0.34$$

$$h_{23} = 0.28$$

$$h_{3j} = 0.25$$

$$h_{21} = 0.56$$

$$h_{32} = 0.41$$

$$h_{ai} = 0.04$$

the values of the coefficients are

$$C_{aw} = 31.89$$

$$\epsilon_w C_{aw} = 0.0209$$

$$C_{aB} = 1.980$$

$$\epsilon_B C_{aB} = 0.0036$$

The analog patching diagram is shown in Figure 8-4.

8.6 Water Drag

The pressure drag is discussed in Section 4.6.2 and it is noted that the drag coefficient would be different depending upon whether the buoy was rising or falling, relative to the water. If the relative velocity is defined as

$$v = \dot{\eta} - \dot{z}_B$$

then when this velocity is positive the drag coefficient would be the forebody drag coefficient and when this velocity is negative it would be the base drag coefficient. Typical values are given in Reference 10, Chapter 3, and are

Forebody	$C_D = 0.90$
Base	$C_D = 0.03$

The analog patching diagrams to generate the drag coefficients and the associated drag forces are shown in Figure 8-5.

8.7 Turbine Torque

The torque produced by the turbine due to the air flow is discussed in Chapter 6. Defining

$$T_t = \text{torque scale factor}$$

$$\Omega_t = \text{turbine angular velocity scale factor}$$

the scaled torque equation is

$$\left[\frac{T}{T_t} \right] = \left(\frac{C_T A_w^2 V^2}{T_t A_j^2} \right) \left[\frac{\dot{z}_A}{V} \right] \left\{ \left[\frac{\dot{z}_A}{V} \right] - \left(\frac{C_s \Omega_t A_j}{V A_w} \right) \left[\frac{\omega}{\Omega_t} \right] \right\}$$

where C_T and C_s are given by equations (6-5), and (6-7). Basic data for the WATG-4 turbine is as follows:

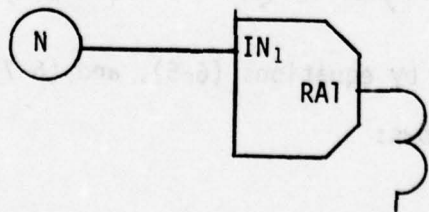
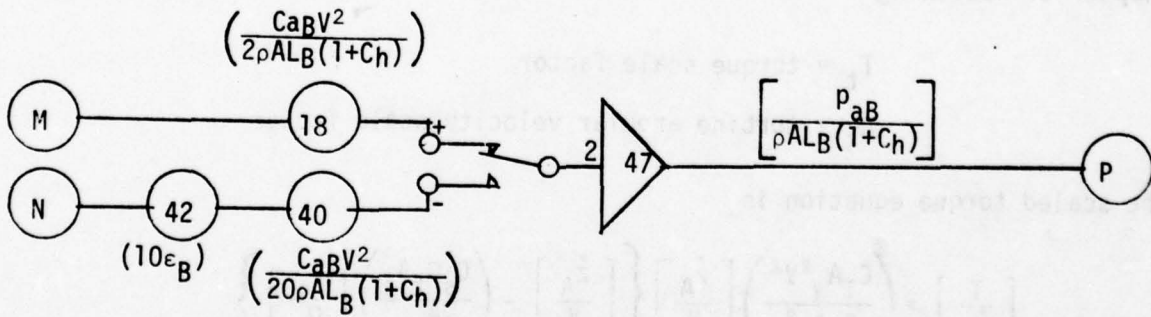
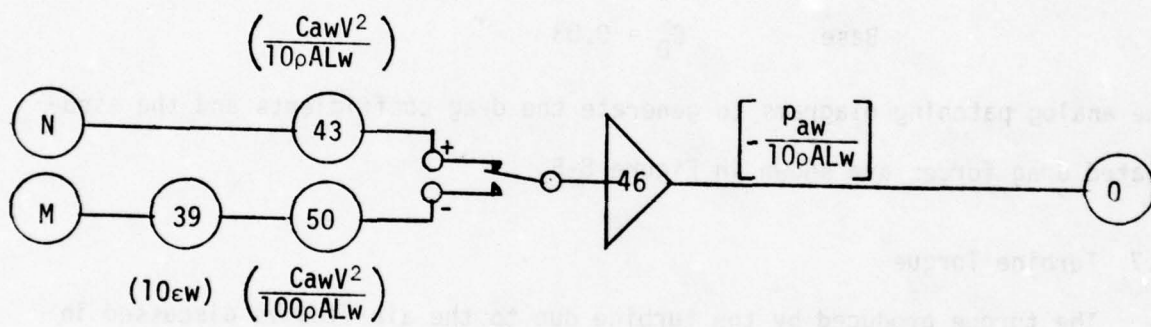
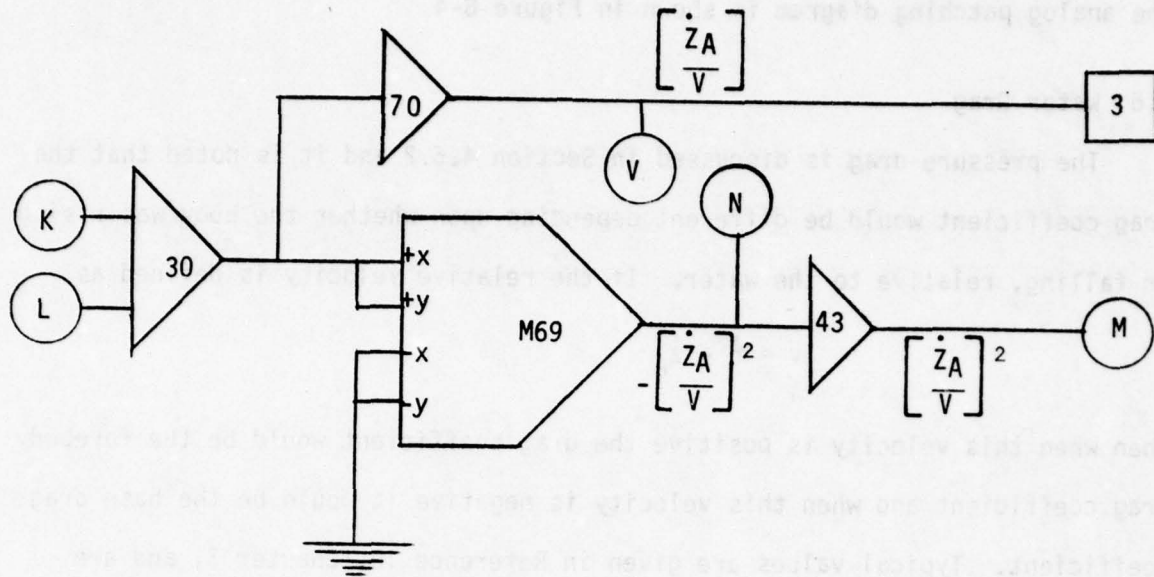


FIGURE 8-4. AIR PRESSURE FORCES

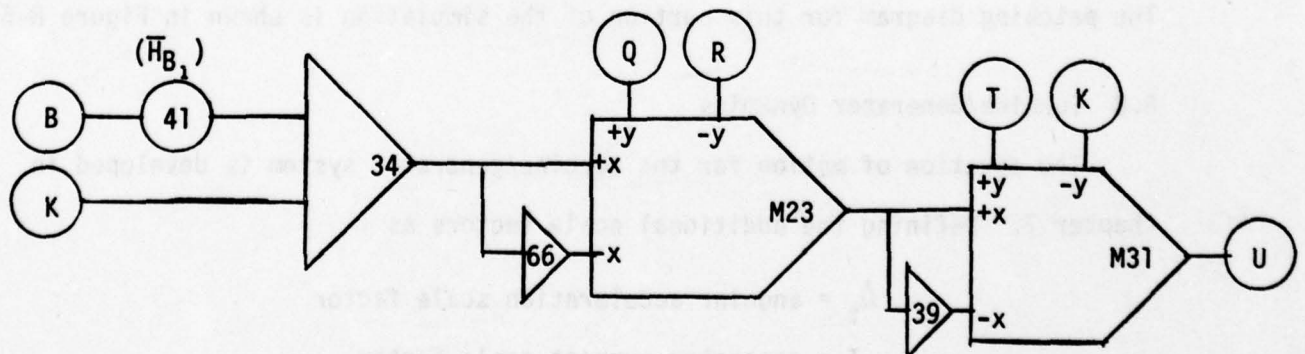
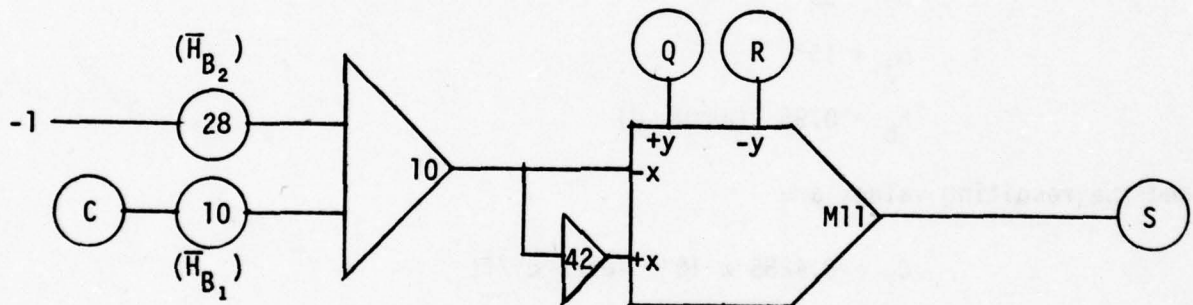
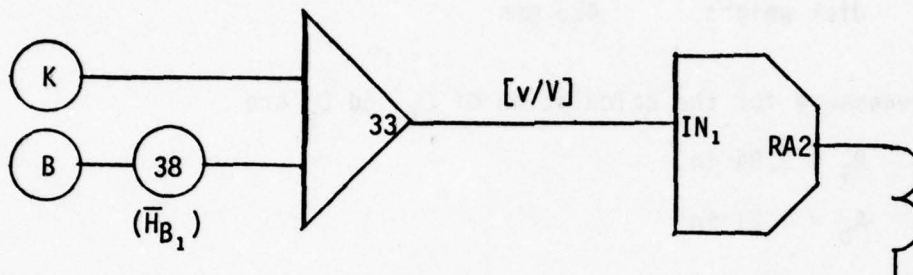
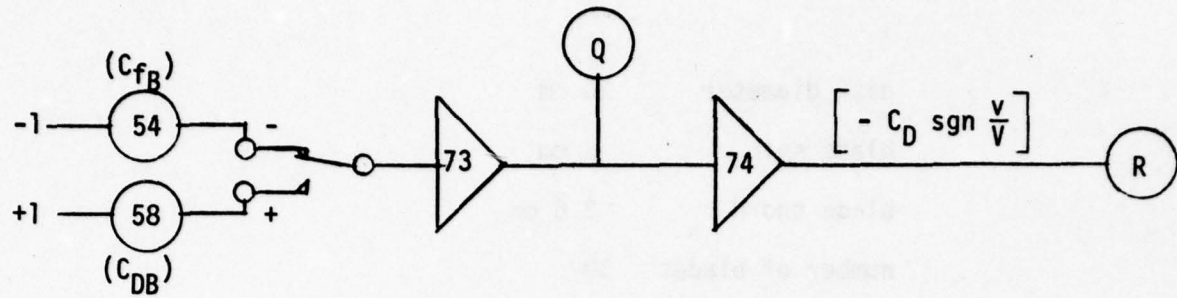


Figure 8-5. WATER DRAG COEFFICIENT AND FORCES

disk diameter	20 cm
blade span	3 cm
blade chord	2.6 cm
number of blades	30
blade spacing	2.09 cm
disk weight	425 gms

The parameters necessary for the calculation of C_T and C_S are

$$R_T = 3.94 \text{ in.}$$

$$A_b = 1.21 \text{ in}^2$$

$$n = 30$$

$$k = 1 \text{ (ref. 8, pg. 183)}$$

$$\beta_2 = 25^\circ$$

$$\alpha_j = 15^\circ$$

$$h_b = 0.95 \text{ (assumed)}$$

and the resulting values are

$$C_T = 0.4285 \times 10^{-4} \text{ lbs-sec}^2/\text{ft}$$

$$C_S = 0.6220 \text{ ft}$$

The patching diagram for this portion of the simulation is shown in Figure 8-6.

8.8 Turbine/Generator Dynamics

The equation of motion for the turbine/generator system is developed in Chapter 7. Defining the additional scale factors as

$$\dot{\Omega}_t = \text{angular acceleration scale factor}$$

$$I = \text{generator current scale factor}$$

the scaled equation of motion is

$$\begin{bmatrix} \dot{\omega} \\ \dot{\Omega}_t \end{bmatrix} = \begin{pmatrix} T_t \\ J\Omega_t \end{pmatrix} \begin{bmatrix} T \\ T_t \end{bmatrix} - \begin{pmatrix} B\Omega_t \\ J\Omega_t \end{pmatrix} \begin{bmatrix} \omega \\ \Omega_t \end{bmatrix} - \begin{pmatrix} k_G I \\ J\Omega_t \end{pmatrix} \begin{bmatrix} i \\ I \end{bmatrix}$$

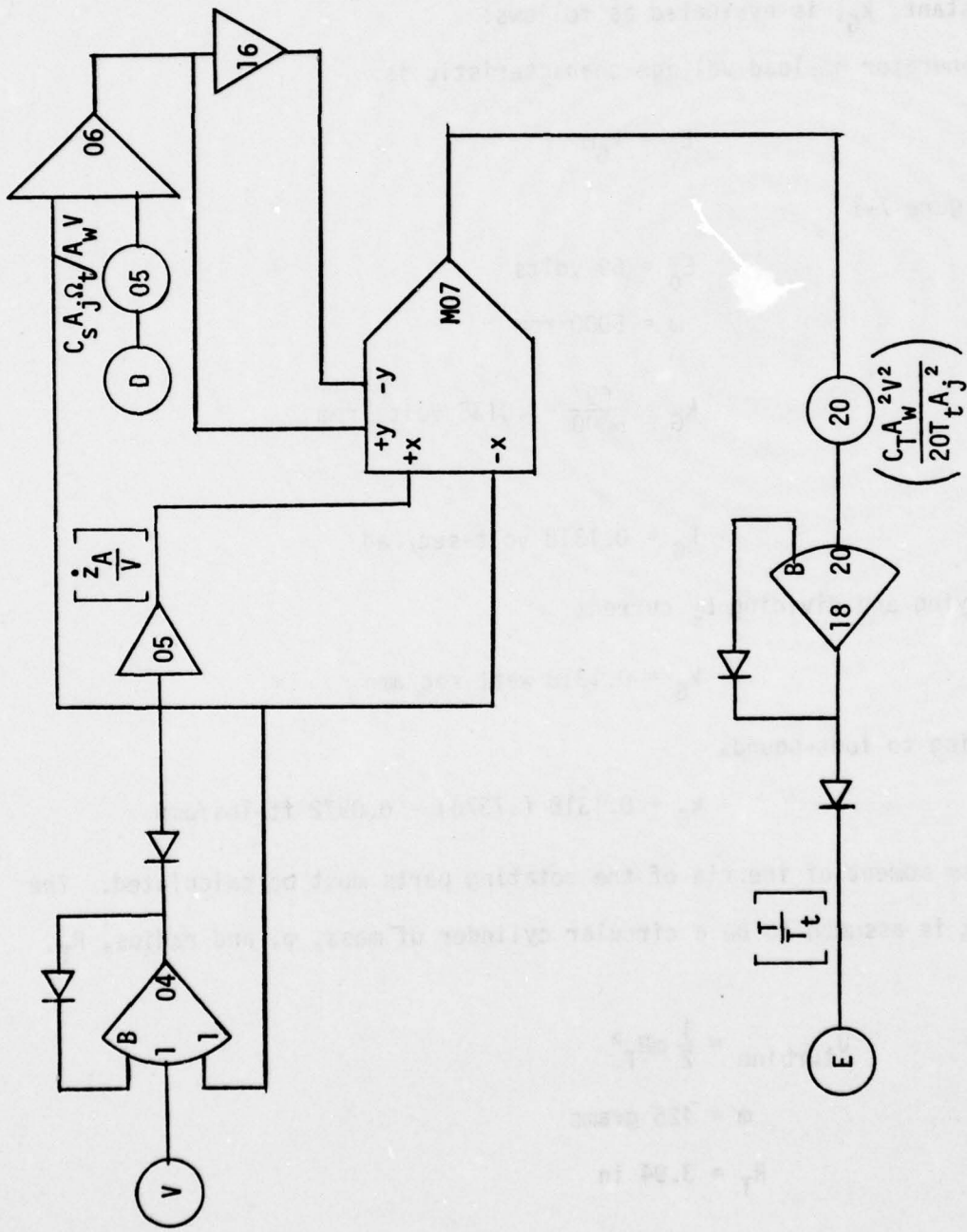


Figure 8-6. TURBINE TORQUE

This equation requires that the generator current versus generator angular velocity be available in the simulation. This relationship is simulated by reproducing Figure 7-1 using a variable diode function generator. The patching diagram for the function generator is shown in Figure 8-7. The generator torque constant, k_G , is evaluated as follows:

The generator no-load voltage characteristic is

$$E_o = k_G \omega$$

and from Figure 7-1

$$E_o = 69 \text{ volts}$$

$$\omega = 5000 \text{ rpm}$$

from which

$$k_G = \frac{69}{5000} = .0138 \text{ volts/rpm}$$

or

$$k_G = 0.1318 \text{ volt-sec/rad}$$

and multiplying and dividing by current

$$k_G = 0.1318 \text{ watt-sec/amp}$$

and converting to foot-pounds

$$k_G = 0.1318 (.7376) = 0.0972 \text{ ft-lbs/amp}$$

The mass moment of inertia of the rotating parts must be calculated. The turbine disk is assumed to be a circular cylinder of mass, m , and radius, R_T , so that

$$J_{\text{turbine}} = \frac{1}{2} m R_T^2$$

$$m = 425 \text{ grams}$$

$$R_T = 3.94 \text{ in}$$

so

$$J_{\text{turbine}} = \frac{1}{2} \left(\frac{425}{454} \right) \left(\frac{1}{32.2} \right) \left(\frac{3.94}{12} \right)^2 = 0.001567 \text{ lb-ft-sec}^2$$

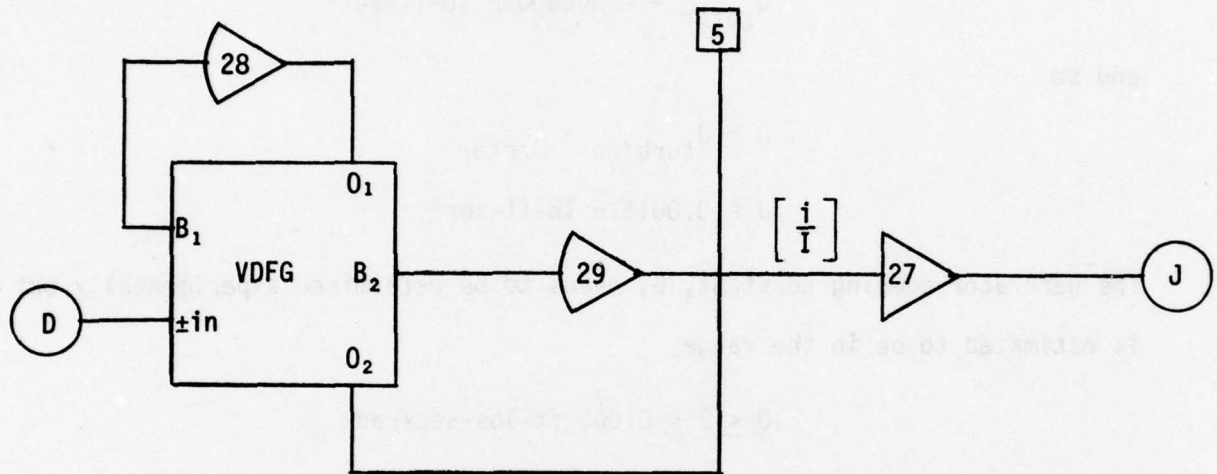


Figure 8-7. GENERATOR CURRENT VS. RPM

The generator rotor is assumed to be a steel cylinder 3/4 inches in diameter and 5 inches long so

$$\begin{aligned} J_{\text{rotor}} &= \frac{1}{2} mR^2 \\ &= \frac{1}{2} (.283) \frac{\pi}{4} (.75)^2 (5) \frac{1}{32.2} \left(\frac{.375}{12}\right)^2 \\ J_{\text{rotor}} &= 0.00000948 \text{ lb-ft-sec}^2 \end{aligned}$$

and so

$$\begin{aligned} J &= J_{\text{turbine}} + J_{\text{rotor}} \\ J &= 0.001576 \text{ lb-ft-sec}^2 \end{aligned}$$

The generator damping constant, B, needs to be determined experimentally but is estimated to be in the range

$$0 \leq B \leq 0.005 \text{ ft-lbs-sec/rad}$$

The patching diagram for the turbine/generator equation of motion is shown in Figure 8-8.

8.9 Parameters for a Typical Simulation

A typical WATG configuration to be analyzed is one with the buoy draft, $L_B = 4$ feet and a water column length, $L_W = 15$ feet. These values correspond to a buoy natural period of 2.8 seconds and a water column natural period of 4.3 seconds. The coefficients presented are for the case where the buoy is forced, by a sinusoidal wave, at its natural period, with a wave height of $H = 1$ foot. The scale factors used are:

$$\begin{aligned} \delta &= 10 \text{ ft} \\ V &= 20 \text{ ft/sec} \\ A &= 50 \text{ ft/sec}^2 \\ \Omega_t &= 500 \text{ rad/sec} \end{aligned}$$

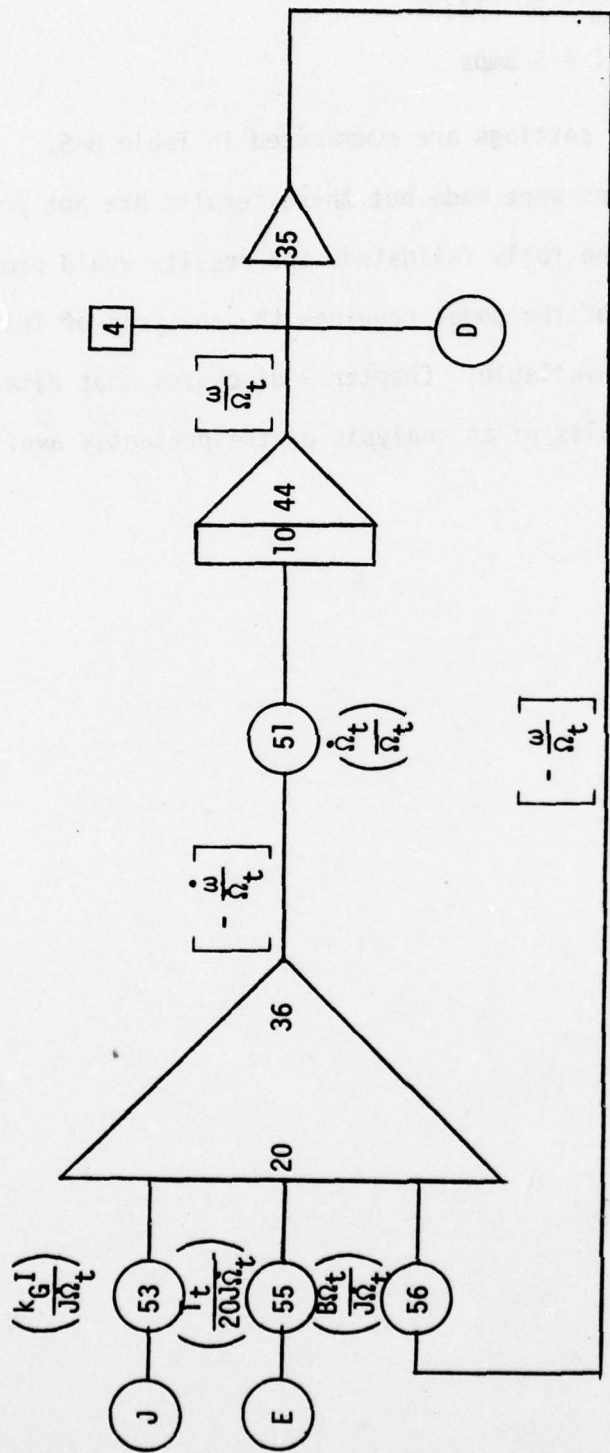


Figure 8-8. TURBINE/GENERATOR EQUATION OF MOTION

$$\dot{\Omega}_t = 1000 \text{ rad/sec}^2$$

$$T_t = 20 \text{ ft-lbs}$$

$$I = 5 \text{ amps}$$

The resulting potentiometer settings are summarized in Table 8-5.

Various simulation runs were made but these results are not presented since, until the model can be fully validated, the results would probably not be meaningful. Validation of the model requires the analysis of full-scale test data which is not yet available. Chapter 9 discusses what data is required and presents the results of an analysis of the presently available data.

Table 8-5. POTENTIOMETER SETTINGS FOR PARAMETERS
GIVEN IN SECTION 8.9

Pot No.	Parameter	Setting	Remarks
00	$\Omega/10$	0.224	Gain of 10, A00
01	$\Omega/10$	0.224	Gain of 10, A01
02	$C_{B\delta}$	0.098	
03	C_{BV_1}	0.273	
05	$C_{Sj} A_{\Omega} / A_w V$	0.106	
06	C_{BV_2}	0.606	
07	$C_{BH_2} \bar{H}_{B_2}$	0.004	
08	$10 C_{Bf}$	0.061	
10	\bar{H}_{B_1}	0.028	
11	$C_{BH_1} \bar{H}_{B_1}$	0.015	
12	$C_{BH_3} \bar{H}_{B_3}$	0.008	
13	constant	0.100	
15	$\Omega/10$	0.224	Gain of 20, A12
16	$\Omega/10$	0.224	Gain of 20, A13
18	$C_{aB} V^2 / 2\rho A L_B (1+C_h)$	0.618	Gain of 2, A47
20	$C_{T_w} A_w^2 V^2 / 20 T_t A_j^2$	0.918	Gain of 20, A18
22	A/V	0.250	Gain of 10, A20
23	V/ δ	0.200	Gain of 10, A21
25	$C_{w\delta} / 10$	0.043	Gain of 10, A22
26	C_{wf}	0.040	
27	\bar{H}_w	0.002	
28	\bar{H}_{B_2}	0.060	
30	$HC_{\eta} / 20$	0.025	Gain of 10, A17

Table 8-5. (continued)

POTENTIOMETER SETTINGS FOR PARAMETERS GIVEN IN SECTION 8.9

Pot No.	Parameter	Setting	Remarks
38	\bar{H}_{B_1}	0.028	
39	$10\epsilon_w$	0.006	
40	$C_{aB} V^2 / 20\rho AL_B (1+C_h)$	0.062	Gain of 2, A47
41	\bar{H}_{B_1}	0.028	
42	$10\epsilon_B$	0.018	
43	$C_{aw} V^2 / 10\rho AL_w$	0.877	
45	A/V	0.250	Gain of 10, A37
46	V/ δ	0.200	Gain of 10, A45
50	$C_{aw} V^2 / 100\rho AL_w$	0.088	
51	$\dot{\Omega}_t / \Omega_t$	0.200	Gain of 10, A44
53	$k_G I / J\dot{\Omega}_t$	0.308	
54	C_{fB}	0.900	
55	$T_t / 20J\dot{\Omega}_t$	0.634	Gain of 20, A36
56	$B\dot{\Omega}_t / J\dot{\Omega}_t$	0.793	
58	C_{DB}	0.030	

9. VALIDATION OF THE SIMULATION MODEL

9.1 Introduction

In dealing with mechanical systems, generally the most troublesome area to simulate realistically is the mechanism of energy dissipation. Usually the dissipation law is not known but assumed, but even if the law is known, the values of the parameters involved are generally not known. Previous work on the WATG assumed only a linear dissipation law but showed that the power produced is sensitive to the value of the dissipation parameter (damping ratio in this case). The present study assumes a combination of linear and second-order dissipation and estimates the values of the parameters involved for both the buoy and the water column. The true dissipation mechanisms and the values of the parameters involved needs to be determined.

The second area involving validation is related to the turbine/generator dynamics. The torque-speed-air velocity relationship was derived in Chapter 6. The true functional relationship needs to be determined and if the equation derived is adequate the values of the parameters C_T and C_S need to be determined. Furthermore, a linear dissipation term and a linear electrical torque term were assumed in the equation of motion and this needs to be validated and quantified.

9.2 Data Requirements

9.2.1 Turbine tests

First, using the generator alone, a no-load test can be conducted wherein the no-load voltage is recorded as a function of time as the generator speed decays from known initial values. Analysis of this data will determine the nature of the mechanical dissipation torque. Second, a similar series of tests,

under load, together with the known relationship between current and RPM, will determine the nature of the electrical dissipation torque. Once these characteristics have been determined the WATG assembly, consisting of the generator, turbine, and air passage can be mounted on a test stand such that known, time-varying air inputs can be introduced. A means to measure the torque delivered at the generator rotor and to measure the generator RPM will provide the data necessary to deduce the torque-speed-air velocity relationship.

9.2.2 Buoy/water column tests

An instrumented buoy is presently deployed and two variables being measured are buoy acceleration and water column displacement relative to the buoy. Analysis of the data being gathered is complicated by the fact that the wave input is variable. If data could be taken in a sheltered area of essentially calm water, a series of step response tests could be run. The buoy would be lifted partially out of the water and released. An analysis of the resulting decay of acceleration and relative displacement would yield the applicable dissipation laws referred to in Section 9.1. Some data similar to this has been accumulated and its analysis is discussed in the next section.

9.3 Analysis of Available Data

9.3.1 Determination of the dissipation law

Step response tests using an 8 x 26 buoy without the WATG and with the center tube closed at the bottom were conducted by the USCG in June and October of 1974. Acceleration versus time was recorded and five such recordings were made available. A typical record is shown in Figure 9-1. The usual procedure to deduce a damping law from such data is to assume a law and then see how well (statistically) the data fits the law. If a linear law is assumed (dissipative force directly proportional to velocity), then a semi-log plot of peak positive

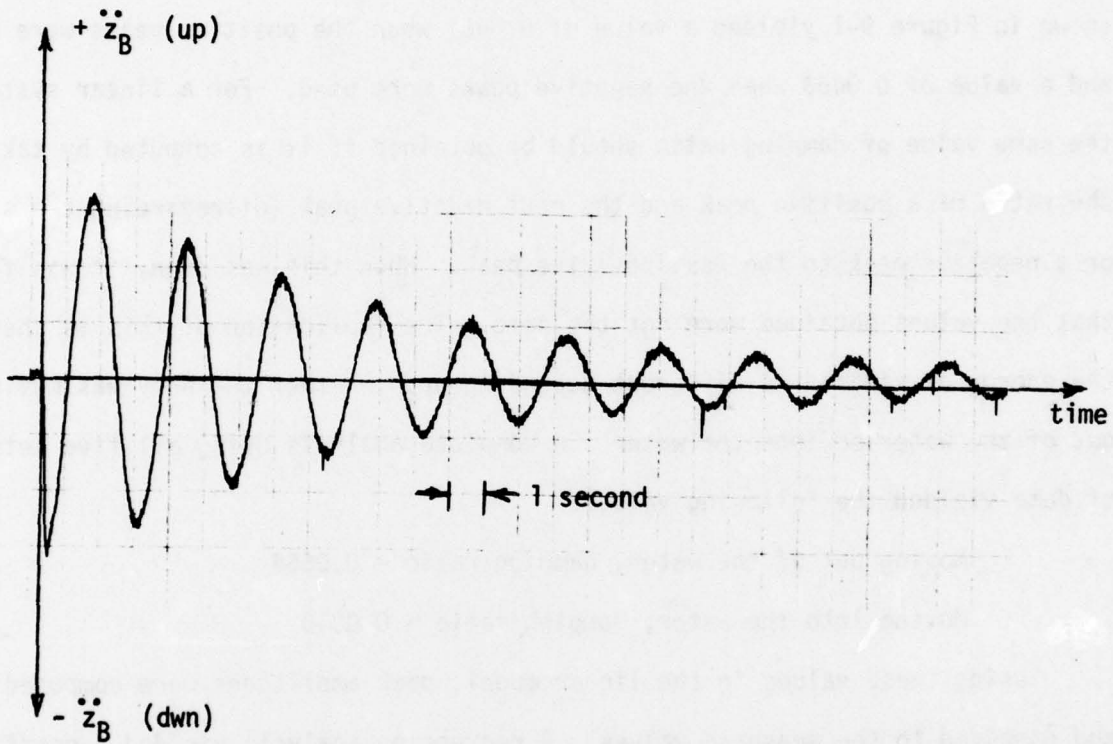


Figure 9-1. BUOY ACCELERATION VS. TIME; STEP RESPONSE
TESTS OF 8 X 26 BUOY

(or negative) amplitudes versus number of cycles should yield a straight line. This was the case for all five data records. The slope of this semi-log plot, multiplied by suitable constants yields the damping ratio. This value can be found by a least squares fit to the line. The results for the particular record shown in Figure 9-1 yielded a value of 0.0461 when the positive peaks were used and a value of 0.0463 when the negative peaks were used. For a linear system the same value of damping ratio should be obtained if it is computed by taking the ratio of a positive peak and the next negative peak (disregarding the sign) or a negative peak to the next positive peak. When this was done, it was found that the values obtained were not the same. The implication of this is that the energy dissipated is different depending upon whether the buoy was moving out of the water or into the water. A complete analysis using all five sets of data yielded the following values:

Moving out of the water, damping ratio = 0.0664

Moving into the water, damping ratio = 0.0319

Using these values in the linear model, peak amplitudes were computed and compared to the measured values. A regression analysis yielded a coefficient of determination greater than 0.99 which means that less than 1% of the difference between the calculated and measured data is not accounted for by the assumed law.

The physical explanation for this behavior would appear to be that when the buoy is moving into the water, viscous forces are generated but when moving out of the water, a wake is developed which generates additional viscous forces. This form of energy dissipation might be termed bilinear viscous damping; the dissipative force being directly proportional to velocity but with the constant of proportionality having one value for positive velocity and another value for negative velocity. Two questions remain with regard to the present simulation;

first, is this law applicable to the buoy when the center pipe is not capped and second, what is the dissipation law for the relative water motion in the center pipe. These questions can be answered by conducting the tests outlined in Section 9.2.2.

9.3.2 Determination of the added mass coefficient

The step response data yields a damped natural period of the buoy tested of 2.7 seconds. Since, as was shown, the damping is small, this can be taken as the undamped natural period. The buoy natural frequency is, therefore,

$$\omega_B = \frac{2\pi}{T} = \frac{2\pi}{2.7} = 2.33 \text{ RAD/SEC}$$

Now, since

$$\omega_B^2 = \frac{g}{L_B(1+C_h)}$$

and, for the buoy tested $L_B = 3.61$ Feet

$$C_h = 0.65$$

which is the value used to calculate the coefficients presented in Chapter 8. Since, for the buoy tested, the center pipe was capped, future tests as proposed in Section 9.2.2 will determine any necessary correction to this value.

9.3.3 Modification of the simulation equations

The validation procedure may require that certain forces in the basic equations be modified or that the numerical value of coefficients used be modified. The forces involved are:

D_{wB} = water column friction force, Section 3.3

D_f = buoy friction force, Section 4.6.1

D_p = buoy pressure force, Section 4.6.2

D_R = buoy radial dissipation force, Section 4.6.3

T = turbine torque, Section 6.2

$B\omega$ = turbine/generator mechanical dissipation torque, Section 7.2

$k_G i$ = turbine/generator electrical dissipation torque, Section 7.2

If the damping law discussed in Section 9.3.1 proves applicable, the simulation equations would be significantly less complex.

10. CONCLUSIONS AND RECOMMENDATIONS

The objectives of this project, as stated in the Introduction, have been met. The buoy, water column, air passage, turbine and generator have been modeled and analog computer patching diagrams presented. The available full scale data has been analyzed and this analysis indicates that modifications in the model will probably be required. This conclusion cannot be made more definite since the data analyzed was for the buoy alone without a water column. It is likely, however, that even with a water column, the dissipation law will be proved to be bilinear thus simplifying the equations as presented herein.

It is recommended that any continuing work on this project include the following:

- (1) The tests of the turbine and generator outlined in Section 9.2.1.
- (2) The buoy/water column tests as outlined in Section 9.2.2.
- (3) Modification of the simulation equations as required by the aforementioned tests.
- (4) Generation of Response Amplitude Operators from the simulation model.
- (5) Comparison of the RAO's generated by the simulation with those to be available from the deployed buoys now under test.
- (6) Presentation of the results in a form suitable for the USCG digital Design Integration Model currently under development.

The possibility exists that analysis of the pure heaving motion may not be adequate to describe the actual buoy behavior. If this should be the case, then the model would have to be modified to include the coupled tilt-heave dynamics.

REFERENCES

1. McCormick, M. E., "Analysis of a Wave Energy Conversion Buoy," J. of Hydronautics, Vol. 8, No. 3, July 1974, pp. 77-82.
2. McCormick, M. E., Carson, B. H., and Rau, D. H., "An Experimental Study of a Wave Energy Conversion Buoy," Marine Techn. Soc. J., Vol. 9, No. 3, March 1975, pp. 39-42.
3. McCormick, M. E., "A Modified Linear Analysis of a Wave Energy Conversion Buoy," USNA Report EW-6-75, May 1975
4. St. Dennis, M., "Floating Hulls Subject to Wave Action," Handbook of Ocean and Underwater Engineering," McGraw-Hill, 1969.
5. Pearson, C. E., Handbook of Applied Mathematics, Van Nostrand, 1974.
6. Tuma, J. J., Engineering Mathematics Handbook, McGraw-Hill, 1970.
7. Swanson, W. M., Fluid Mechanics, Holt, Rinehart, Winston, 1970.
8. Shepherd, D. G., Principles of Turbomachinery, MacMillan, 1956.
9. Bolz, R. E., and Tuve, G. L., Handbook of Tables for Applied Engineering Science, CRC Press, 1973.
10. Hoerner, S. F., Fluid Dynamic Drag, 1958.